AGU100 ADVANCING EARTH AND SPACE SCIENCE

Radio Science

RESEARCH ARTICLE
10.1029/2018RS006584

Key Points:
- The weighted intercept probability and transmit power of radar networks is defined and used as the LPI performance optimization criterion
- To support LPI optimization, a JTSRM strategy is developed and then formulated as an optimization problem
- We build a closed-loop JTSRM framework for target tracking in distributed radar networks

Correspondence to:
C. G. Shi and F. Wang,
scg_space@163.com;
wangxiaoxian@nuaa.edu.cn

Citation:
Shi, C. G., Wang, F., Salous, S., & Zhou, J. J. (2018). Joint transmitter selection and resource management strategy based on low probability of intercept optimization for distributed radar networks. *Radio Science*, *53*, 1108–1134. https://doi.org/10.1029/2018RS006584

Received 20 MAR 2018
Accepted 18 JUL 2018
Accepted article online 2 AUG 2018
Published online 17 SEP 2018

Joint Transmitter Selection and Resource Management Strategy Based on Low Probability of Intercept Optimization for Distributed Radar Networks

C. G. Shi[1], F. Wang[1], S. Salous[2], and J. J. Zhou[1]

[1] Key Laboratory of Radar Imaging and Microwave Photonics, Ministry of Education, Nanjing University of Aeronautics and Astronautics, Nanjing, China, [2] School of Engineering and Computing Sciences, Durham University, Durham, UK

Abstract In this paper, a joint transmitter selection and resource management (JTSRM) strategy based on low probability of intercept (LPI) is proposed for target tracking in distributed radar network system. The basis of the JTSRM strategy is to utilize the optimization technique to control transmitting resources of radar networks in order to improve the LPI performance while guaranteeing a specified target-tracking accuracy. The weighted intercept probability and transmit power of radar networks is defined and subsequently employed as the optimization criterion for the JTSRM strategy. The resulting optimization problem is to minimize the LPI performance criterion of radar networks by optimizing the revisit interval, dwell time, transmitter selection, and transmit power subject to a desired target-tracking performance and some resource constraints. An efficient and fast three-step solution technique is also developed to solve this problem. The presented mechanism implements the optimal working parameters based on the feedback information in the tracking recursion cycle in order to improve the LPI performance for radar networks. Numerical simulations are provided to verify the superior performance of the proposed JTSRM strategy.

1. Introduction

1.1. Background and Motivation

Distributed radar network systems, which are also known as spatial distributed multiple-input multiple-output radar and multistatic radar (Haimovich et al., 2008; Li & Stoica, 2009; Pace, 2009), have attracted significant attention and are on the path from theory to practical use. The radar networks incorporating multiple transmitters and multiple receivers work cooperatively to achieve a specified task. It has been demonstrated that these systems have a number of performance advantages over monostatic radar owing to its waveform diversity, spatial diversity, and multiplexing gain, which have triggered a resurgence of interest in radar network systems. Due to the rapid developments in large bandwidth wireless networks, multichannel electronically scanned antennas, high-speed low-cost processors, and precise synchronization system, the implementation of radar network has become feasible and it will be deployed more widely in the near future (Pace, 2009). Hence, considerable research has been conducted into the potential use of such networks for achieving network performance improvement in various contexts such as target detection (Fisher et al., 2006; Naghsh et al., 2013), target localization (Niu et al., 2012), target tracking (Godrich et al., 2012), waveform design (Y. F. Chen et al., 2013; Nguyen et al., 2015), sensor selection (Shi, Wang, Sellathurai, et al., 2016), and information extraction (Song et al., 2012).

Since low probability of intercept (LPI) design has been an essential and important part of military operations in hostile environments (Lynch, 2004; Schleher, 2006; Shi et al., 2018), the concept of resource-aware management, aiming to efficiently minimize the transmitting resources consumption while maintaining a desired performance requirement, has been studied extensively. In this paper, we investigate the problem of joint transmitter selection and resource management (JTSRM) strategy for distributed radar networks. The objective of JTSRM optimization strategy is to minimize the defined LPI performance criterion for radar networks by optimally scheduling the working parameters of the whole network.

In order to improve LPI performance, it is necessary to dynamically design the radar resources while guaranteeing a specified target tracking accuracy. Technically speaking, low transmit power, short dwell time, large revisit interval, ultra-low side lobe antenna, and waveform agility will lead to better LPI performance (Lynch,

2004). The problem of LPI-based radar resource-aware design in traditional monostatic radars has been extensively studied from various perspectives, where the transmit power, dwell time, and revisit interval of the radar transmitter for the next time index are calculated based on the obtained target state estimation to maintain a predefined tracking performance. In 1993, Keuk and Blackman (1993) investigated the problem of phased-array radar tracking and parameter control and optimized beam scheduling, signal-to-noise ratio (SNR), and detection threshold to reduce the radiated energy. Then, Daeipour et al. (1994) presented an adaptive sampling method to track the highly maneuvering targets with an interacting multiple model (IMM) estimator. However, the algorithm of Daeipour et al. (1994) did not consider false alarms and electronic counter measurements, Blair et al. (1998) extended the results in Daeipour et al., (1994) and proposed a benchmark problem for adaptive beam-pointing control of a phased-array radar in the presence of false alarms and electronic counter measurements. Later, the authors in Kirubarajan et al. (1998) developed a set of algorithms for radar management and maneuvering target tracking, whose main contribution was that it integrated target tracking and radar management and provided a unified framework for these two aspects. The aforementioned works mainly focused on adaptive sampling and transmitted power control scheme, while the problem of time budget spent on the target was studied by Zwaga et al. (2003) for the first time, and the total dwell time spent for guaranteeing a given tracking accuracy is minimized. Furthermore, the optimization problem of Zwaga et al. (2003) was upgraded in Boers et al. (2006) and reformulated an efficient strategy without an additional constraint on the probability of detection. In Wang et al. (2017), Wang et al. propose a joint revisit and dwell time management strategy for single-target tracking based on the predicted Bayesian Cramer-Rao lower bound in-phased-array radar system, where the resource burden is minimized with the target-tracking performance, meeting a specified threshold. Also, LPI-based radar resource-aware design for target tracking has been addressed in multiple-target tracking (Zhang et al., 2011) and multisensor selection scenarios (J. Chen et al., 2014; Kalandros & Pao, 2002; Puranik & Tugnait, 2005).

Overall, the reported studies demonstrate that adaptive transmitting parameters management is an effective technique to improve the LPI performance of radar systems. Although the reported works provide us a guidance to deal with the problem of LPI optimization for target tracking, they are all focused on the monostatic radar. Applying this idea to the radar networks case will face many technical challenges, which is because the radar network performance depends not only on the transmitted parameters but also on the relative geometry between target and radar network configuration.

1.2. Brief Survey of Similar Work

In recent years, the LPI optimization-based resource-aware management for target tracking in radar network systems has been preliminarily investigated, which can be classified into two categories. The first aspect of resource management is the optimal allocation of the available transmit power. In this case, the total transmit power is minimized by optimizing power allocation among netted radar nodes for a specified target-tracking accuracy (Shi et al., 2014), where most of the available power is assigned the radars with better propagation path conditions. In the second case, the radar with the minimum resource burden in the network is selected for next observation at each time index (Narykov et al., 2013; Narykov & Yarovoy, 2013), which aims at optimizing the revisit interval and dwell time of the selected radar for LPI requirement. Zhang et al. (2015) proposed a cooperation algorithm of radar network system for multiple-target tracking in clutter, where the radar with the minimum transmitted power is selected for better LPI performance. As an extension, Zhang and Tian (2016) developed a resource-scheduling scheme, whose basis is to adjust the revisit interval, transmit power, and carrier frequency of the selected radar, with the purpose of minimizing the transmitted power of radar network. In practical scenario, owing to the limitations on transmission rate, communication bandwidth, and LPI performance, only a few radar nodes are available at any given time (Xie et al., 2018). In addition, the specified mission requirements may be accomplished by utilizing a part of the radar nodes. The authors in She et al. (2016, 2017) study the problem of LPI-based joint sensor selection and power allocation for multiple-target tracking in radar networks, whose purpose is to minimize the total transmitted power of the networks by optimizing sensor selection and power allocation for a predefined target estimation performance, while the transmitting parameters, such as revisit interval and dwell time, are not optimized. Thus, the resulting LPI performance may not be the optimum. In Shi et al. (2017), Shi et al. develop an LPI-based adaptive resource management scheme for target tracking in radar networks, which is composed of one dedicated radar transmitter and multiple receivers. The basis is to adjust the revisit interval, dwell time, and transmit power of the dedicated transmitter by employing the information fed back from the tracker, with the purpose of improving the LPI performance of radar networks. However, the active radar transmitter is fixed

such that its transmitting power is not always the minimum in the networks, and the upper convex property of the intercept probability with respect to the dwell time is not analytically proved. Therefore, resource management and radar transmitter selection should be taken into consideration at the same time. Above all, to the best of the authors' knowledge, the problem of how to optimize the working parameters in terms of the revisit interval, dwell time, transmitter selection, and transmit power to improve the LPI performance of radar networks, which is the focus of this paper, has not yet been fully considered until now.

In this work, we extend the existing publications and present a JTSRM strategy for target tracking in distributed radar networks. Overall, it is more practical and important based on the above (Xie et al., 2018). A closed-loop LPI-based JTSRM framework is built for target tracking in a radar network system. We utilize the predictive information obtained from the tracking recursion cycle to implement the optimal transmitter selection and resource management. To be specific, the objective of LPI-based JTSRM optimization considered in this paper is to minimize the defined LPI performance metric by optimizing the revisit interval, dwell time, transmitter selection, and transmit power of the overall system subject to a desired target-tracking accuracy and several resource constraints. The optimization results are sent back to the system controller to form the next illumination strategy. Hence, the overall network can be viewed as a reaction to the environment, based on which it designs transmitting resources optimally.

1.3. Main Contributions

The major contributions of this paper are summarized as follows:

1. *The weighted intercept probability and transmit power of radar networks is defined and exploited as the LPI performance optimization criterion for the JTSRM strategy*, which incorporates the revisit interval, dwell time, transmitter selection, and transmit power of overall system. To gauge the LPI performance, it is common to employ the well-known intercept probability (Lynch, 2004). Previously, the resource management work in Shi et al. (2017) utilizes the intercept probability of radar networks as the objective function. However, although the intercept probability is minimized, the transmit power of the overall system is not always the minimum. Thus, it is reasonable for us to define a novel weighted intercept probability and transmit power as the optimization criterion.
2. *To support LPI optimization, a JTSRM strategy is developed and then formulated as an optimization problem:* Mathematically speaking, the JTSRM strategy is a problem of optimizing a cost function about the LPI performance of radar networks subject to a certain performance requirement and some resource constraints (Yan et al., 2016). With the defined LPI performance criterion, the basis of the JTSRM strategy is to optimally control the revisit interval, dwell time, transmitter selection, and transmit power of overall system, which leads to the minimization of the LPI performance criterion.
3. *Implementing the LPI performance-driven methods into real-time systems necessitates the quick and efficient calculation of the optimization problem. To achieve this goal, we develop an efficient and fast three-step solution to solve the resulting JTSRM optimization problem:* First, we utilize an adaptive selection method for the revisit interval to determine the revisit interval for the next time index. Then, we strictly prove that the intercept probability is upper convex with respect to the dwell time, and thus, the optimal solution can be obtained at the boundary. After that, the radar node with the minimum transmit power is selected to illuminate the target in the next time period.
4. *We build a closed-loop JTSRM framework for target tracking in distributed radar networks:* In this work, the IMM-extended Kalman filter (EKF) algorithm is employed to obtain an accurate target state estimation at the current time index. At the same time, the predictive information obtained from the tracking recursion cycle is utilized to form the illumination strategy. After that, the probing strategy for the next time index can be obtained by implementing the developed three-step solution approach to the resulting optimization problem. The optimization results are then sent back to the radar networks to guide the illumination strategy for the next time index, thereby rendering it a closed-loop system. Because of the unique feature of the electronically scanned phased-array radar, the problem of multitarget tracking can be simplified as several single-target-tracking problems that can be solved independently (Xie et al., 2018). Generally, the system model of the closed-loop JTSRM framework is illustrated in Figure 1.

1.4. Outline of the Paper and Notations

The current paper defines a novel LPI performance metric to present a more complete resource-scheduling framework for target tracking in distributed radar networks. Moreover, this study reports on detailed numerical simulations to verify the effectiveness of the proposed JTSRM strategy. The rest of this paper is structured

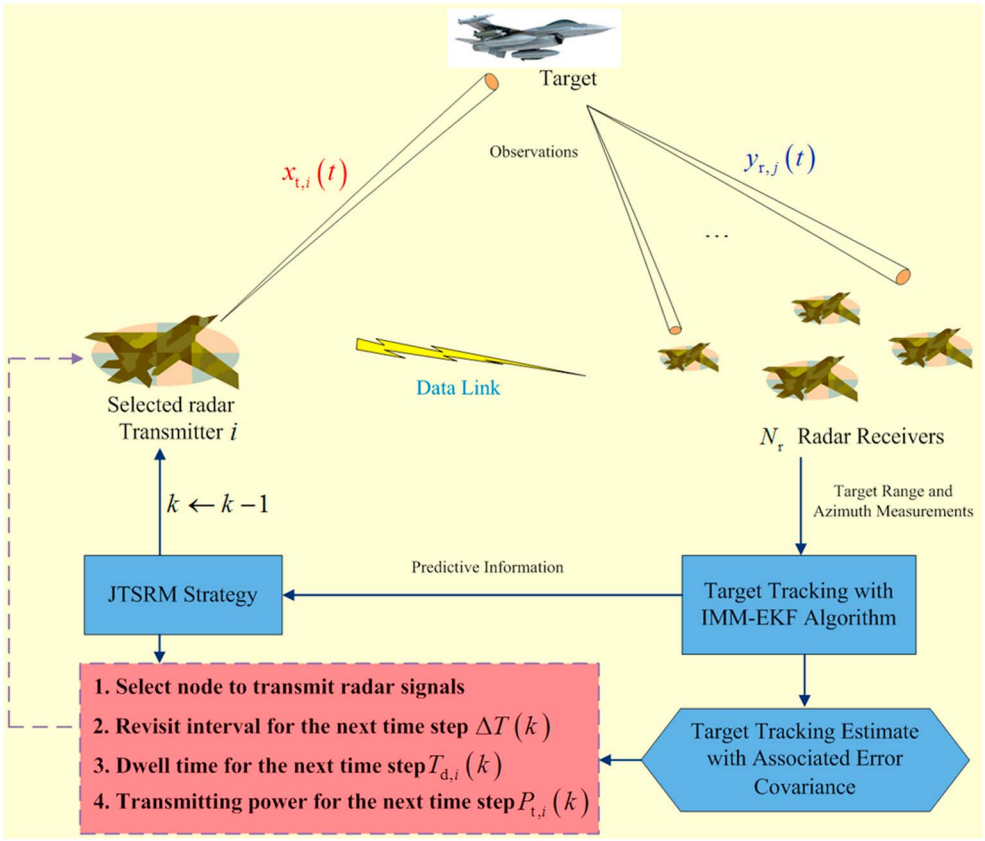

Figure 1. Flow of the closed-loop JTSRM framework for target tracking in distributed radar networks. JTSRM = joint transmitter selection and resource management; IMM = interacting multiple model algorithm; EKF = extended Kalman filter.

as follows: Section 2 introduces the considered system model, and the JTSRM strategy is formulated in section 3. In section 3.1, the basis of the optimization scheme is introduced. Section 3.2 derives the intercept probability of radar networks. The JTSRM optimization problem and the proposed three-step solution technique are presented in sections 3.3 and 3.4, respectively. Section 3.5 summarizes the closed-loop JTSRM framework and some remarks. Several numerical simulations are provided in section 4 to demonstrate the effectiveness of the presented JTSRM scheme. Finally, section 5 concludes this paper.

Notations. The superscript T represents the vector/matrix transpose operator, $\mathbb{E}\{\cdot\}$ represents the expectation operator; $\min\{a, b\}$ denotes the smaller value between a and b; $\mathrm{diag}\{a, b, \ldots, g\}$ denotes a diagonal matrix with diagonal elements $a, b, \ldots, g$; and $\mathrm{tr}[\cdot]$ represents the trace of a matrix.

2. System Model

2.1. Signal Model

Let us consider a radar network system consisting of N_r radar nodes, spatially distributed over a large area as depicted in Figure 1. The distributed radar networks is intended to track the single target with a JTSRM optimization strategy. To facilitate the following derivations, we introduce a binary variable $u_i \in \{0, 1\}$:

$$u_i = \begin{cases} 1, & \text{if the target is illuminated by the } i\text{th radar transmitter,} \\ 0, & \text{otherwise.} \end{cases} \tag{1}$$

At each time index, only one radar node is selected to transmit the Gaussian with linear frequency modulation signal $x_{t,i}(t)(i = 1, 2, \ldots, N_r)$ (Kelly et al., 1996) and all the radars in the networks can receive and process the echoes $y_{r,j}(t)(j = 1, 2, \ldots, N_r)$ scattered off the target. In the following we assume that the radar network has a common precise knowledge of space and time, which means that a fully coherent radar network is considered (Teng et al., 2007). The estimates of time delay, Doppler shift, and arrival angle can be obtained

from all the receivers, where time delay and Doppler shift are estimated employing matched filters and square law envelope detectors, and arrival angle is estimated utilizing phased-array antennas. Then, radar estimates can be sent to the system control center that incorporates a fusion processor to perform joint target tracking and classification and transmitting resource management. The radar network can be broken into $1 \times N_r$ transmitter-receiver pairs, each with a bistatic component contributing to the entirety of the radar network SNR. Hence, the radar network can be considered as a connected series of bistatic radar systems. On the one hand, a bistatic target radar cross section (RCS) for each transmitter-receiver pair must be calculated; on the other hand, it is assumed that the thermal noise at each receiver is statistically independent. For convenience, the radar nodes are labeled as $\mathbb{S} = \{1, 2, \ldots, N_r\}$, with the locations of the ith radar transmitter being denoted by $(x_{t,i}, y_{t,i})$ and the jth receiver being denoted by $(x_{r,j}, y_{r,j})$, respectively. Therefore, the overall radar network SNR can be obtained by summing up the SNR of each transmit-receive pair as follows:

$$\begin{aligned} \mathrm{SNR}_{\mathrm{net}} &= \sum_{j=1}^{N_r} \mathrm{SNR}_j \\ &= \sum_{j=1}^{N_r} \frac{u_i P_{t,i} G_{t,i} G_{r,j} \sigma_j \lambda^2 G_{\mathrm{RP}}}{(4\pi)^3 k T_0 B_{r,j} F_{r,j} R_t^2 R_{r,j}^2}, \end{aligned} \tag{2}$$

where SNR_j denotes the SNR at the jth receiver, $P_{t,i}$ denotes the peak transmitted power of the selected radar transmitter i, $G_{t,i}$ is the ith transmitting antenna gain, G_r is the jth receiving antenna gain, σ_j represents the target RCS for the selected radar transmitter and jth receiver, λ represents the transmitted wavelength, G_{RP} denotes the radar network processing gain, k and T_0 are Boltzmann's constant and the receiving system noise temperature, respectively, $B_{r,j}$ denotes the bandwidth of the matched filter for the transmitted waveform at the jth receiver, $F_{r,j}$ denotes the noise factor for the jth receiver, $R_{t,i}$ and $R_{r,j}$ are the distance between the ith radar transmitter and target, and the distance between the target and the jth receiver, respectively.

Furthermore, the following assumptions are summarized to simplify the optimization problem (Xie et al., 2018).

1. *Assumption 1:* It is assumed that the target is known from the radar search mode, and the tracks are initialized by employing the maximum likelihood-probabilistic data association approach.
2. *Assumption 2:* Each radar operates in a multiple-input multiple-output mode, which can not only receive its own signal echo but also receive and process the target echoes transmitted by other radar nodes.
3. *Assumption 3:* The radar network system has good connectivity. That is, there exists a multiloop communication route connecting any pair of radar nodes in the networks.

2.2. Target Dynamic Model

Set ΔT as the measurement revisit interval for target tracking. Then, the time index $k\Delta T$ can be denoted as k. Considering a two-dimensional target-tracking scenario, the target model is a discrete-time dynamical motion model of the following form:

$$\mathbf{X}(k) = \mathbf{F}\mathbf{X}(k-1) + \mathbf{W}(k-1), \tag{3}$$

where $\mathbf{X}(k) = [x(k), \dot{x}(k), y(k), \dot{y}(k)]^T$ is the target state vector at time index k, $[x(k), y(k)]$ denotes the target position, and $[\dot{x}(k), \dot{y}(k)]$ denotes the target velocity. $\mathbf{F}$ is the state transition matrix. The process noise $\mathbf{W}(k-1)$ in (3) represents a white Gaussian random process with a known covariance matrix $\mathbf{Q}(k-1) = \mathbb{E}[\mathbf{W}(k-1)\mathbf{W}(k-1)^T]$, which is given by

$$\mathbf{Q}(k-1) = \sigma_w^2 \begin{bmatrix} \frac{\Delta T^4}{4} & \frac{\Delta T^3}{2} & 0 & 0 \\ \frac{\Delta T^3}{2} & \Delta T^2 & 0 & 0 \\ 0 & 0 & \frac{\Delta T^4}{4} & \frac{\Delta T^3}{2} \\ 0 & 0 & \frac{\Delta T^3}{2} & \frac{\Delta T^4}{4} \end{bmatrix}, \tag{4}$$

where σ_w^2 represents a process noise intensity corresponding to the level of target maneuverability.

2.3. Measurement Model

Let the kinematic measurement corresponding to the selected transmitter i at time index k be denoted as $\mathbf{Z}(k)$. Then, the nonlinear measurement vector of target state at time index k can be given by

$$\mathbf{Z}^i(k) = \begin{cases} \mathbf{h}^i(\mathbf{X}(k)) + \mathbf{V}^i(k), & u_i(k) = 1, \\ 0, & u_i(k) = 0. \end{cases} \tag{5}$$

where $\mathbf{Z}^i(k)$ is the measurement vector corresponding to the selected transmitter i at time index k, $\mathbf{h}^i(\cdot)$ represents the nonlinear transformation from the target state vector of target position in Cartesian coordinates to the measurement vector of time delay and azimuth angle (Nguyen et al., 2015), and $u_i(k)$ denotes the binary variable u_i at time index k. The measurement noise $\mathbf{V}^i(k)$ is a white Gaussian random process, independent of $\mathbf{W}(k)$, with zero mean value and covariance matrix $\mathbf{R}^i(k)$:

$$\mathbf{R}^i(k) = \operatorname{diag} \underbrace{\left\{ \mathbf{R}^i_1(k), \mathbf{R}^i_2(k), \ldots, \mathbf{R}^i_{N_r}(k) \right\}}_{N_r}, \tag{6}$$

where $\mathbf{R}^i_j(k)$ denotes the error covariance matrix at the jth receiver. Here the measurement vector $\mathbf{Z}^i(k)$ includes time delay measurement $\tau^i_j(k)$ with respect to each receiver and associated arrival angle measurement $\theta^i_j(k)$. Without loss of generality, we assume that the selected radar transmitter i is located at $(x_{t,i}, y_{t,i})$ and the jth receiver is located at $(x_{r,j}, y_{r,j})$, respectively. Thus, when $u_i(k) = 1$, (5) can be rewritten as

$$\mathbf{Z}^i(k) = \begin{bmatrix} \tau^i_1(k) \\ \theta^i_1(k) \\ \vdots \\ \tau^i_{N_r}(k) \\ \theta^i_{N_r}(k) \end{bmatrix} + \mathbf{V}^i(k) = \begin{bmatrix} \frac{1}{c_v}\left(\sqrt{\left[x(k) - x_{t,i}\right]^2 + \left[y(k) - y_{t,i}\right]^2} + \sqrt{\left[x(k) - x_{r,1}\right]^2 + \left[y(k) - y_{r,1}\right]^2} \right) \\ \arctan\left(\frac{y(k) - y_{r,1}}{x(k) - x_{r,1}} \right) \\ \vdots \\ \frac{1}{c_v}\left(\sqrt{\left[x(k) - x_{t,i}\right]^2 + \left[y(k) - y_{t,i}\right]^2} + \sqrt{\left[x(k) - x_{r,N_r}\right]^2 + \left[y(k) - y_{r,N_r}\right]^2} \right) \\ \arctan\left(\frac{y(k) - y_{r,N_r}}{x(k) - x_{r,N_r}} \right) \end{bmatrix} + \mathbf{V}^i(k), \tag{7}$$

where c_v is the speed of light.

Following Kershaw and Evans (1994) and Sira et al. (2007), it is assumed that the side lobes of the ambiguity function can be neglected with high SNR and the errors in the radar estimates can achieve the Cramer-Rao lower bounds (CRLBs). In addition, since the errors at different receivers are statistically independent from each other, we employ the results in Kershaw and Evans (1994) and set $\mathbf{R}^i(k)$ equal to the CRLB $\mathbf{B}^i(k)$ shown as follows:

$$\mathbf{B}^i(k) = \operatorname{diag} \underbrace{\left\{ \mathbf{B}^i_1(k), \mathbf{B}^i_2(k), \ldots, \mathbf{B}^i_{N_r}(k) \right\}}_{N_r}, \tag{8}$$

with

$$\mathbf{B}^i_j(k) = \frac{1}{\mathrm{SNR}_{j,\mathrm{pre}}(k)} \begin{bmatrix} \frac{c_v^2 \tau^2}{2} & 0 \\ 0 & \sigma_\theta^2 \end{bmatrix}, \tag{9}$$

where $\mathbf{B}^i_j(k)$ denotes the CRLB of the estimates at receiver j, $\mathrm{SNR}^i_{j,\mathrm{pre}}(k)$ denotes the predicted target SNR at receiver j for time index k (which is expressed in section 3.4), τ is the pulse width, and σ_θ^2 is the variance of the measurement noise in azimuth.

Remark 1: It should also be pointed out that we consider the target tracking in a two-dimensional Cartesian space for simplicity, which can easily be extended to the three-dimensional space. In the presence of multiple targets, the numbers of target states and measurements are increased by a factor equal to the number of targets, making the analysis and derivations much more complex. In the target-tracking application, target dynamics are usually modeled in the Cartesian coordinates, while target measurements are directly available in the polar or spherical coordinate. When the radar measurements are converted to the ones in the Cartesian coordinate by some measurement conversion techniques, the target dynamic model can be used in the engineering application.

2.4. IMM-EKF Algorithm

2.4.1. EKF Algorithm

The key to target tracking lies in the effective extraction of useful kinematic information about the target state from observations. An effective model will certainly facilitate this information extraction to a great extent. From section 2.2 and section 2.3, the discrete-time form of differential model can depict the target kinematic motion. For the nonlinear measurements of target state, the standard EKF algorithm is utilized to track the target with a single-target dynamic model, which can achieve a better trade-off between the target-tracking performance and computational cost than linear Kalman filter and unscented Kalman filter. The necessary EKF recursive equations are provided as follows:

1. *Prediction:*

$$\hat{\mathbf{X}}(k|k-1) = \mathbf{F}\hat{\mathbf{X}}(k-1|k-1), \tag{10}$$

$$\mathbf{P}(k|k-1) = \mathbf{F}\mathbf{P}(k-1|k-1)\mathbf{F}^T + \mathbf{Q}(k-1), \tag{11}$$

$$\mathbf{S}^i(k) = \mathbf{H}^i(k)\mathbf{P}(k|k-1)(\mathbf{H}^i(k))^T + \mathbf{R}^i(k), \tag{12}$$

2. *Update:*

$$\mathbf{K}^i(k) = \mathbf{P}(k|k-1)\mathbf{H}^i(k)(\mathbf{S}^i(k))^{-1}, \tag{13}$$

$$\widetilde{\mathbf{Z}}^i(k) = \mathbf{Z}^i(k) - \mathbf{h}^i(\hat{\mathbf{X}}(k|k-1)), \tag{14}$$

$$\hat{\mathbf{X}}(k|k) = \hat{\mathbf{X}}(k|k-1) + \mathbf{K}^i(k)\widehat{\mathbf{Z}}^i(k), \tag{15}$$

$$\mathbf{P}(k|k) = \left[\mathbf{I} - \mathbf{K}^i(k)\mathbf{H}^i(k)\right]\mathbf{P}(k|k-1), \tag{16}$$

where $\hat{\mathbf{X}}(k|k-1)$ and $\mathbf{P}(k|k-1)$ are the state vector's a priori estimate and covariance matrix, respectively. $\mathbf{S}^i(k)$ is the innovation covariance, and $\mathbf{K}^i(k)$ is the filter gain matrix. $\mathbf{I}$ is an identity matrix. $\hat{\mathbf{X}}(k|k)$ and $\mathbf{P}(k|k)$ are the state vector's a posteriori estimate and covariance matrix, respectively. The matrix $\mathbf{H}^i(k)$ is a Jacobian of $\mathbf{h}^i(\hat{\mathbf{X}}(k|k-1))$ for time index k evaluated in $\hat{\mathbf{X}}(k|k-1)$ as follows:

$$\mathbf{Z}^i(k) = \frac{\partial \mathbf{h}^i(\hat{\mathbf{X}}(k|k-1))}{\partial \hat{\mathbf{X}}(k|k-1)} \tag{17}$$

$$= \begin{bmatrix} \frac{1}{c_v}\left(\frac{x(k|k-1)-x_{t,i}}{R_{t,i}(k|k-1)} + \frac{x(k|k-1)-x_{r,1}}{R_{r,1}(k|k-1)}\right) & \frac{1}{c_v}\left(\frac{y(k|k-1)-y_{t,i}}{R_{t,i}(k|k-1)} + \frac{y(k|k-1)-y_{r,1}}{R_{r,1}(k|k-1)}\right) & 0\ 0 \\ -\frac{y(k|k-1)-y_{r,1}}{R^2_{r,1}(k|k-1)} & -\frac{x(k|k-1)-x_{r,1}}{R^2_{r,1}(k|k-1)} & 0\ 0 \\ \vdots & \vdots & \vdots\ \vdots \\ \frac{1}{c_v}\left(\frac{x(k|k-1)-x_{t,i}}{R_{t,i}(k|k-1)} + \frac{x(k|k-1)-x_{r,N_r}}{R_{r,N_r}(k|k-1)}\right) & \frac{1}{c_v}\left(\frac{y(k|k-1)-y_{t,i}}{R_{t,i}(k|k-1)} + \frac{x(k|k-1)-x_{r,N_r}}{R_{r,N_r}(k|k-1)}\right) & 0\ 0 \\ -\frac{y(k|k-1)-y_{r,N_r}}{R^2_{r,N_r}(k|k-1)} & -\frac{x(k|k-1)-x_{r,N_r}}{R^2_{r,N_r}(k|k-1)} & 0\ 0 \end{bmatrix}, \tag{18}$$

where

$$\begin{cases} R_{t,i}(k|k-1) = \sqrt{\left[x(k|k-1) - x_{t,i}\right]^2 + \left[y(k|k-1) - y_{t,i}\right]^2}, \\ R_{r,j}(k|k-1) = \sqrt{\left[x(k|k-1) - x_{r,j}\right]^2 + \left[y(k|k-1) - y_{r,j}\right]^2}, \end{cases} \tag{19}$$

are the distance predictions between the selected radar transmitter i and target and between the target and the jth receiver, respectively.

2.4.2. Interacting Multiple Model

The standard EKF algorithm is sufficient to track the target with a single-target dynamic model. However, for the target with time-varying or multiple dynamic models, a single dynamic model cannot represent the actual target motion well. For that reason, we employ the IMM method incorporating three target dynamic models in this paper: (a) a constant velocity model $\mathbf{F}_{CV}$, (b) a coordinate turn model $\mathbf{F}_{CT}$ with positive turn rate w_+, and (c) a coordinate turn model $\mathbf{F}_{CT}$ with negative turn rate w_-, which are given by

$$\mathbf{F}_{CV} = \begin{bmatrix} 1 & 0 & \Delta T & 0 \\ 0 & 1 & 0 & \Delta T \\ 0 & 0 & 1 & 0 \\ 0 & 0 & 0 & 1 \end{bmatrix}, \tag{20}$$

$$\mathbf{F}_{CT} = \begin{bmatrix} 1 & \frac{\sin(w\Delta T)}{w} & 0 & \frac{\cos(w\Delta T)-1}{w} \\ 0 & \cos(w\Delta T) & 0 & \sin(w\Delta T) \\ 0 & \frac{1-\cos(w\Delta T)}{w} & 1 & \frac{\sin(w\Delta T)}{w} \\ 0 & \sin(w\Delta T) & 0 & \cos(w\Delta T) \end{bmatrix}, \tag{21}$$

where w is the turn rate.

The IMM method can estimate the target state with three tracking filters running in parallel, where each tracking filter is responsible for a particular target dynamic model, and finally obtain a weighted combination of the state estimates and tracking covariances from individual tracking filters (Nguyen et al., 2015). For the update cycle at time index k, the target state estimate $\hat{\mathbf{X}}_i(k-1|k-1)$, the state error covariance $\mathbf{P}_i(k-1|k-1)$, and the model probability $q_i(k-1)$ corresponding to each filter can be obtained from the previous cycle at time index $k-1$. This information and the measurement vector $\mathbf{Z}(k)$ are utilized to update the IMM parameters at time index k.

The crucial feature of the JTSRM strategy in radar networks is that it must be predictive. The predicted error covariance matrix enables the decision making in advance based on current knowledge. Given the predicted target state $\hat{\mathbf{X}}_i(k|k-1)$, model probability $q_i(k|k-1)$, and error covariance matrix $\mathbf{P}_i(k|k-1)$ at time index, the combined target state $\widehat{\mathbf{X}_{\text{pre}}^{\text{IMM}}}(k|k-1)$ and error covariance matrix $\mathbf{P}_{\text{pre}^{\text{IMM}}}(k|k-1)$ can be calculated by

$$\hat{\mathbf{X}}_{\text{pre}}^{\text{IMM}}(k|k-1) = \sum_{i=1}^{3} q^i(k|k-1)\hat{\mathbf{X}}_i(k|k-1), \tag{22}$$

$$\begin{aligned} \mathbf{P}_{\text{pre}}^{\text{IMM}}(k|k-1) = \sum_{i=1}^{3} q_i(k|k-1)\{\mathbf{P}_i(k|k-1) + [\hat{\mathbf{X}}_i(k|k-1) - \hat{\mathbf{X}}_{\text{pre}}^{\text{IMM}}(k|k-1)] \\ \times [\hat{\mathbf{X}}_i(k|k-1) - \hat{\mathbf{X}}_{\text{pre}}^{\text{IMM}}(k|k-1)]^T\}. \end{aligned} \tag{23}$$

Note that $\hat{\mathbf{X}}_{\text{pre}}^{\text{IMM}}(k|k-1)$ and $\mathbf{P}_{\text{pre}}^{\text{IMM}}(k|k-1)$ are the predicted target state and error covariance for time index k given measurements through time $k-1$.

3. JTSRM Strategy

3.1. Basis of the Technique

Mathematically, the proposed JTSRM strategy for target tracking in radar networks can be formulated as a problem of minimizing the LPI performance criterion subject to a certain target-tracking performance and some resource constraints.

In this paper, the adaptable parameters are the revisit interval, dwell time, transmitter selection, and transmit power. The weighted intercept probability and transmit power of radar networks incorporate the revisit interval, dwell time, transmitter selection, and transmit power of overall system, which thus is defined and employed as the LPI optimization criterion for the resource management strategy. The predicted target state and error covariance matrix calculated in the previous section are utilized to form the illumination strategy for the next time step. We are then in a position to minimize the LPI performance metric by optimizing the working parameters in order to achieve better LPI performance. The developed JTSRM strategy is detailed as follows.

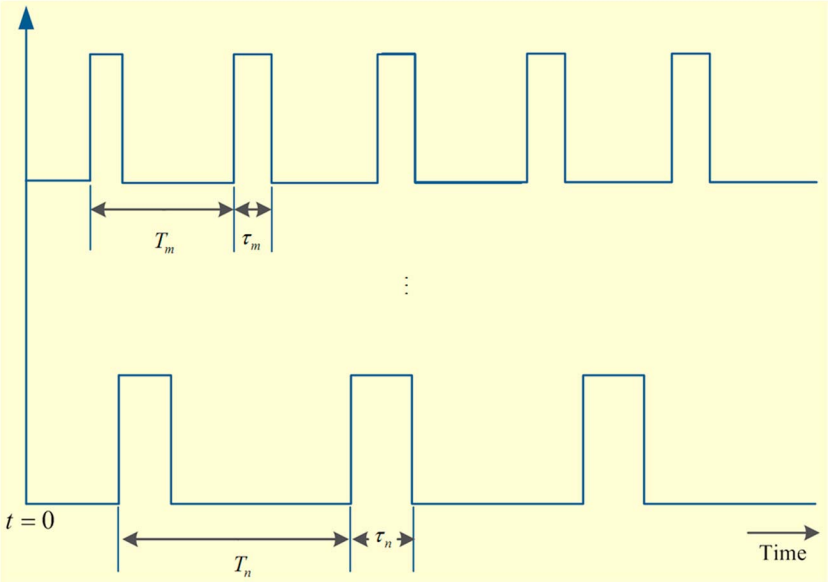

Figure 2. Window function model.

3.2. Intercept Probability of Radar Networks

As indicated in Lynch (2004) and Pace (2009), the best LPI strategy is to not radiate at all. However, the radar systems need to perform several tasks, such as target detection, target localization, target tracking, and classification. Thus, the next best LPI strategy is to manage the radiated energy. Power management is defined as the ability to adjust the power level emitted by the radar transmitter and control the radiated power to a predetermined target detection requirement. In addition, the dwell time should also be limited.

In this paper, it is supposed that the intercept receiver is carried by the target for simplicity, which can be an omnidirectional radar warning receiver that has full 360° coverage over a wide range of frequency. The interception of the radar transmission can quickly result in electronic attack or jamming, if the transmitting parameters of the radar are determined (Pace, 2009). With energy control, the radar transmitter emits the minimum energy for target tracking. As the range to target is decreased, the received energy at the intercept receiver reduces, which can force the radar warning receiver into incorrectly placing its priorities for electronic attack. That is to say, due to the decrease of the intercepted energy, the intercept receiver on board the target may identify the radar as nonthreatening, and thereby, no attack or jamming is necessary.

Intercept probability is widely utilized to evaluate LPI performance for radar systems. Based on the model in Self and Smith (1985) and Wiley (2006), intercept probability is shown to be a function of several variables, such as the time-on-target, intercept receiver search time, and transmitted power. The intercept probability depends on the joint probability of the spatial domain, frequency domain, time domain, and power domain. Window function provides a good model to investigate the intercept problem (Self & Smith, 1985), which can represent the activities of the radar transmitter and intercept receiver systems in each domain. Figure 2 shows two window functions, which have respective window periods T_m, T_n and window durations τ_m, τ_n. Given that the received signal at the intercept receiver is above its detection threshold, the intercept probability relates to the probability of time coincidence of two or more parametric windows in different domains.

As aforementioned, the interceptor system uses an omnidirectional antenna, together with a step-scan receiver to search the frequency band B_I in M_I steps, so that it is unnecessary to search the radar signal in azimuth. It is also assumed that the radar transmitter is fixed in frequency. Thus, only two windows need to be considered, that is, transmitter spatial scanning and intercept receiver frequency scanning.

In the general case, it is reasonable to assume that both windows are independent with each other. For a step-scan receiver, the duration of frequency scan in each step can be given by

$$\tau_I = \frac{M_I}{B_I} T_I, \tag{24}$$

where T_I denotes the intercept receiver total search time. When the radar network tracks the target during the dwell time $T_{d,i}$ of selected transmitter i, the main beam of the dedicated transmitter illuminates the omnidirectional intercept receiver. Then, the mean period of simultaneous overlaps of two window junctions is expressed as

$$T_M = \frac{\frac{T_I}{\tau_I}\frac{\Delta T}{T_{d,i}}}{\frac{1}{\tau_I}+\frac{1}{T_{d,i}}}, \tag{25}$$

where ΔT is the revisit interval. Hence, the spatial-time-frequency intercept probability that an intercept occurs during the time $T_{d,i}$ can be obtained as follows (Shi et al., 2017; Yan et al., 2016):

$$p_{stf} = 1 - K_0 \exp\left(-\frac{T_{d,i}}{T_M}\right), \tag{26}$$

where

$$K_0 = 1 - \frac{T_I}{\tau_I}\frac{\Delta T}{T_{d,i}} = 1 \tag{27}$$

since $\tau_I \ll T_I$ and $T_{d,i} \ll \Delta T$.

The probability that the interceptor detects the radar-transmitted signal when it is above the threshold of the intercept receiver is $p_d^{'}$, which refers to the probability that the radar network is detected assuming beam illumination and proper frequency tuning. With the derivations in Mahafza and Elsherbeni (2009) and Shi et al. (2016), we can obtain

$$p_d^{'} = \frac{1}{2}\mathrm{erfc}\left(\sqrt{-\ln p_{fa}^{'}} - \sqrt{\mathrm{SNR}_O + \frac{1}{2}}\right), \tag{28}$$

$$\mathrm{erfc}(z) = 1 - \frac{2}{\sqrt{\pi}}\int_0^z e^{-v^3}\mathrm{d}v, \tag{29}$$

where $p_{fa}^{'}$ represents the probability of false alarm, and SNR_O represents the SNR of a single pulse at the intercept receiver output.

The signal power achieved at the intercept receiver from the radar system is

$$P_I = \frac{u_i P_{t,i} G_{t,i}^{'} G_I \lambda^2 G_{IP}}{(4\pi)^2 R_{t,i}^2}, \tag{30}$$

where $G_{t,i}^{'}$ is the ith radar's transmitting antenna gain in the direction of the interceptor, G_I is the gain of the interceptor's antenna, and G_{IP} is the interceptor processing gain. Here the intercept receiver detects the radar main lobe, then $G_{t,i}^{'} = G_{t,i}$. In addition, the sensitivity in the interceptor is

$$S_I = kT_0 B_I F_I(\mathrm{SNR}_O), \tag{31}$$

where F_I denotes the intercept receiver noise factor. Thus, the SNR of a single pulse at the intercept receiver output can be given by

$$\mathrm{SNR}_O = \frac{P_I}{kT_0 B_I F_I} = \frac{u_i P_{t,i} G_{t,i} G_I \lambda^2 G_{IP}}{(4\pi)^2 R_{t,i}^2 kT_0 B_I F_I}. \tag{32}$$

For any fixed value of the probability of false alarm $p_{fa}^{'}$, (28) is derived as

$$p_{\mathrm{d}}^{'}=\frac{1}{2}\mathrm{erfc}\left(\sqrt{-\ln p_{\mathrm{fa}}^{'}}-\sqrt{\frac{u_i P_{\mathrm{t},i} G_{\mathrm{t},i} G_{\mathrm{I}} \lambda^2 G_{\mathrm{IP}}}{(4\pi)^2 R_{\mathrm{t},i}^2 k T_0 B_{\mathrm{I}} F_{\mathrm{I}}}+\frac{1}{2}}\right). \tag{33}$$

Therefore, when the radar transmitter illuminates the intercept receiver, the intercept probability of a radar network can be expressed as follows:

$$\begin{aligned} p_{\mathrm{I}} &= p_{\mathrm{stf}} p_{\mathrm{d}}^{'} = \left[1-K_0 \exp\left(-\frac{T_{\mathrm{d},i}}{T_{\mathrm{M}}}\right)\right] \times \frac{1}{2}\mathrm{erfc}\left(\sqrt{-\ln p_{\mathrm{fa}}^{'}}-\sqrt{\frac{u_i P_{\mathrm{t},i} G_{\mathrm{t},i} G_{\mathrm{I}} \lambda^2 G_{\mathrm{IP}}}{(4\pi)^2 R_{\mathrm{t},i}^2 k T_0 B_{\mathrm{I}} F_{\mathrm{I}}}+\frac{1}{2}}\right) \\ &= \left\{1-\exp\left[-\frac{T_{\mathrm{d},i}(T_{\mathrm{d},i}+\tau_{\mathrm{I}})}{T_{\mathrm{I}} \Delta T}\right]\right\} \times \frac{1}{2}\mathrm{erfc}\left(\sqrt{-\ln p_{\mathrm{fa}}^{'}}-\sqrt{\frac{u_i P_{\mathrm{t},i} G_{\mathrm{t},i} G_{\mathrm{I}} \lambda^2 G_{\mathrm{IP}}}{(4\pi)^2 R_{\mathrm{t},i}^2 k T_0 B_{\mathrm{I}} F_{\mathrm{I}}}+\frac{1}{2}}\right) \\ &\simeq \frac{T_{\mathrm{d},i}(T_{\mathrm{d},i}+\tau_{\mathrm{I}})}{2 T_{\mathrm{I}} \Delta T} \times \frac{1}{2}\mathrm{erfc}\left(\sqrt{-\ln p_{\mathrm{fa}}^{'}}-\sqrt{\frac{u_i P_{\mathrm{t},i} G_{\mathrm{t},i} G_{\mathrm{I}} \lambda^2 G_{\mathrm{IP}}}{(4\pi)^2 R_{\mathrm{t},i}^2 k T_0 B_{\mathrm{I}} F_{\mathrm{I}}}+\frac{1}{2}}\right) \end{aligned} \tag{34}$$

Remark 2: In this paper, we assume that the parameters of intercept receiver, such as interceptor total search time, frequency band, and receiving antenna gain, can be obtained based on military intelligence and prior knowledge. In the simulations, these parameters are set as the typical values of intercept receiver (Lynch, 2004; Wiley, 2006).

Remark 3: In this paper, a key assumption is that the window functions are not in synchronism with each other, which means that the values of starting time are independent of each other. It is indicated in Kelly et al. (1996) that an intercept may not occur if the period of transmitter spatial scanning is harmonically related to that of interceptor frequency scanning. However, in realistic scenarios, the precise starting time of frequency scanning in intercept receiver is usually unavailable. This is because the intercept receiver system does not radiate any radio frequency signals and works passively. Thus, we consider a more general case here.

In the next subsection, we will define a novel LPI optimization metric for evaluating the LPI performance of radar networks, which will be exploited as the optimization criterion in the JTSRM scheme formulated subsequently.

3.3. Problem Formulation

In this subsection, the LPI performance metric is defined as the weighted intercept probability of radar networks p_{I} and the transmit power of selected transmitter $P_{\mathrm{t},i}$ for one step horizon:

$$L(k) \triangleq w_1 \cdot 10\lg[p_{\mathrm{I}}(k)] + w_2 \cdot u_i(k) P_{\mathrm{t},i}(k), \tag{35}$$

where w_1 and w_2 are the weighting factors, $p_{\mathrm{I}}(k)$ is the predicted intercept probability of radar networks for time index k, and $P_{\mathrm{t},i}(k)$ is the transmit power of the selected transmitter for time k. The defined $L(k)$ is taken as the optimization criterion for the JTSRM strategy. Note that $L(k)$ relates to the revisit interval, dwell time, transmitter selection, and transmit power of the whole system. Intuitively, the overall minimum value of $L(k)$ results in the selection of the most suitable revisit interval with the associated optimal transmitting parameters, which in turn means better LPI performance. It should also be noticed that the range to target and arrival angle at the next time index can be predicted by the tracker. Thus, the LPI optimization criterion in (32) can provide guidance to the problem of JTSRM strategy for radar network architecture.

In this paper, the primary objective is to formulate the JTSRM optimization problem, whose purpose is to minimize the LPI performance criterion by optimizing the revisit interval, dwell time, transmitter selection and transmit power with the target-tracking accuracy meeting a predefined threshold P_{th}. Consequently, the underlying JTSRM optimization for target tracking in a distributed radar network system can be formulated as

$$\min_{\Delta T(k), T_{\mathrm{d},i}(k), u_i(k), P_{\mathrm{t},i}(k)} L(k), \tag{36a}$$

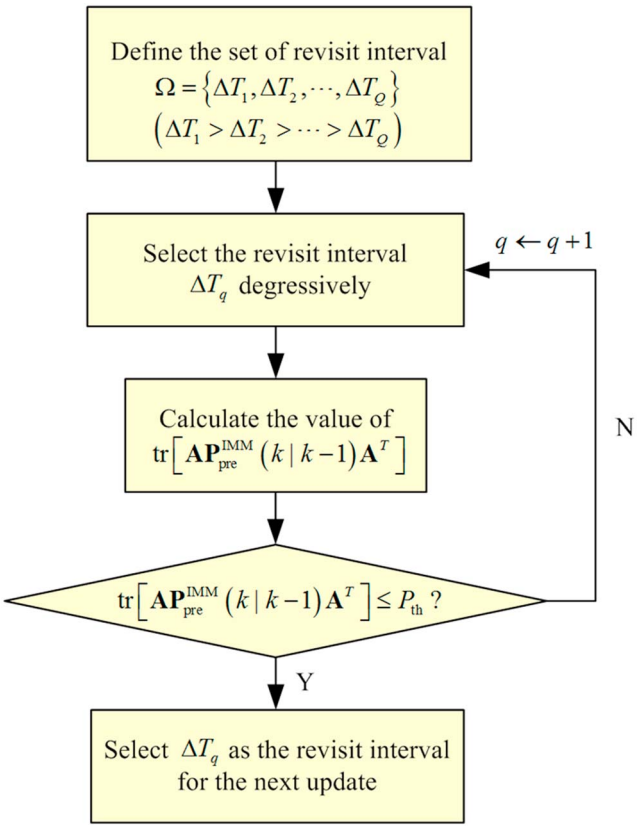

Figure 3. The selection method of the revisit interval.

$$s.t.:\begin{cases}\mathrm{tr}\left[\mathbf{A}\mathbf{P}_{\mathrm{pre}}^{\mathrm{IMM}}(k|k-1)\mathbf{A}^T\right] \le P_{\mathrm{th}},\\ \mathrm{SNR}_{\mathrm{pre}}(k) \ge \mathrm{SNR}_{\mathrm{min}},\\ \Delta T(k) \in \mathbf{\Omega} = \{\Delta T_1, \Delta T_2, \ldots, \Delta T_Q\},\\ \begin{cases} T_{\mathrm{r}} \le T_{\mathrm{d},i}(k) \le \overline{T_{\mathrm{max}}}, u_i(k) = 1,\\ T_{\mathrm{d},i}(k) = 0, u_i(k) = 0, \end{cases}\\ \begin{cases} \overline{P_{\mathrm{min}}} \le P_{\mathrm{t},i}(k) \le \overline{P_{\mathrm{max}}}, u_i(k) = 1,\\ P_{\mathrm{t},i}(k) = 0, u_i(k) = 0, \end{cases} \end{cases} \tag{36b}$$

where $\Delta T(k)$ is the predicted revisit interval for the next update after the measurement at time $k-1$, and $\mathrm{SNR}_{\mathrm{pre}}(k)$ is the predicted SNR of the overall networks for time index k. $\mathbf{A}$ is an auxiliary matrix defined as

$$\mathbf{A} = \begin{bmatrix} 1 & 0 & 0 & 0 \\ 0 & 0 & 1 & 0 \end{bmatrix}, \tag{37}$$

P_{th} is the predefined threshold for target tracking accuracy, the revisit interval $\Delta T(k)$ for the next update is selected from a predefined set of revisit intervals $\mathbf{\Omega} = \{\Delta T_1, \Delta T_2, \ldots, \Delta T_Q\}$, $\mathrm{SNR}_{\mathrm{min}}$ denotes the SNR threshold for target detection performance. The transmit power of the selected radar transmitter i for time k is constrained by a maximum value $\overline{P_{\mathrm{max}}}$ and a minimum value $\overline{P_{\mathrm{min}}}$, and dwell time is constrained by a maximum value $\overline{T_{\mathrm{max}}}$ and the pulse repetition interval T_{r}. It should be noticed from the first constraint in (36a) that the target position accuracy is selected to be the requirement that is applied on the predicted tracking performance (Narykov et al., 2013). The predicted target tracking accuracy is defined as the trace of the 2×2 matrix, $\mathbf{A}\mathbf{P}_{\mathrm{pre}}^{\mathrm{IMM}}(k|k-1)\mathbf{A}^T$, obtained from (23) by keeping only the elements related to the target position variances.

3.4. Problem Partition

From the above derivations, it can be seen that the revisit interval is determined by the predicted error covariance matrix of target state, that is, tr $\left[\mathbf{A}\mathbf{P}_{\text{pre}}^{\text{IMM}}(k|k-1)\mathbf{A}^T\right]$, while the working parameters are related to the measurement error covariance matrix $\mathbf{R}^i(k)$ and overall SNR. Therefore, the revisit interval and working parameters of the whole networks can be solved independently (Cheng et al., 2013; Narykov et al., 2013). In what follows, we approach the problem of JTSRM optimization as a three-step iterative algorithm: the first step is for the selection of revisit interval, the second step is for the scheduling of the working parameters (dwell time, transmitter selection, and transmit power), and finally, the obtained measurement is utilized to update the target state. The general JTSRM optimization strategy is detailed as follows.

3.4.1. Selection of Revisit Interval

The adaptive selection approach of the revisit interval proposed in Daeipour et al. (1994) is utilized in this paper. The next revisit interval is selected from a predetermined set of revisit intervals $\mathbf{\Omega} = \{\Delta T_1, \Delta T_2, \ldots, \Delta T_Q\}$, where $\Delta T_1 > \Delta T_2 > \ldots > \Delta T_Q$, and Q is the total number of the elements in Ω. The revisit interval is selected based on the predicted value of target tracking accuracy, that is, tr $\left[\mathbf{A}\mathbf{P}_{\text{pre}}^{\text{IMM}}(k|k-1)\mathbf{A}^T\right]$. At time index k, the tracker predicts the value of tr $\left[\mathbf{A}\mathbf{P}_{\text{pre}}^{\text{IMM}}(k|k-1)\mathbf{A}^T\right]$ for the largest revisit interval. If the value of tr $\left[\mathbf{A}\mathbf{P}_{\text{pre}}^{\text{IMM}}(k|k-1)\mathbf{A}^T\right]$ is not greater than P_{th} for revisit interval $\Delta T_q (1 \le q \le Q)$, ΔT_q is selected as the revisit interval for the next update and $\Delta T(k)$ is fixed at ΔT_q. Otherwise, the candidate revisit interval is rejected and the test is repeated for the next largest revisit interval ΔT_{q+1}. The selection procedure of the revisit interval is shown in Figure 3. In addition, a variety of schemes for adaptive revisit interval selection can be applied and their references are provided in Kalandros and Pao (2002).

3.4.2. Working Parameters Scheduling

Next, given the revisit interval $\Delta T(k)$, the dwell time $T_{\text{d},i}(k)$, transmitter selection $u_i(k)$, and transmit power $P_{\text{t},i}(k)$ for time index k can be determined. With the overall SNR equation for radar network expressed in (2), the predicted SNR for time k can be calculated as

$$\begin{aligned}\text{SNR}_{\text{pre}}(k) &= \sum_{j=1}^{N_\text{r}} \text{SNR}_{\text{pre},j}(k) \\ &= \sum_{j=1}^{N_\text{r}} \frac{u_i(k)P_{\text{t},i}(k)G_{\text{t},i}G_{\text{r},j}\sigma_j\lambda^2 G_{\text{RP}}}{(4\pi)^3 kT_0 B_{\text{r},j}F_{\text{r},j}R_{\text{t},i}^2(k|k-1)R_{\text{r},j}^2(k|k-1)}.\end{aligned} \tag{38}$$

When the radar network illuminates and tracks a single target during the time $T_{\text{d},i}(k)$, several pulses will be scattered from the target. The process of summing up all the radar echoes available from a target can significantly improve the SNR for a radar network. Here we employ the coherent integration method.

If N_p pulses, with the same SNR, are perfectly integrated by an ideal lossless integrator, the integrated SNR would be exactly N_p times that of a single pulse, given by

$$\text{SNR}_\text{c}(k) = N_\text{p}\text{SNR}_{\text{pre}}(k), \tag{39}$$

where $\text{SNR}_\text{c}(k)$ denotes the integrated SNR of N_p pulses for time index k. Let T_r be the pulse repetition interval, we can then obtain

$$T_{\text{d},i}(k) = N_\text{p}T_\text{r}. \tag{40}$$

Substituting (40) into (39), indicates that

$$\text{SNR}_\text{c}(k) = \frac{T_{\text{d},i}(k)}{T_\text{r}}\text{SNR}_{\text{pre}}(k), \tag{41}$$

Thus, (41) can be calculated as follows:

$$\text{SNR}_\text{c}(k) = \frac{T_{\text{d},i}(k)}{T_\text{r}} \sum_{j=1}^{N_\text{r}} \frac{u_i(k)P_{\text{t},i}(k)G_{\text{t},i}G_{\text{r},j}\sigma_j\lambda^2 G_{\text{RP}}}{(4\pi)^3 kT_0 B_{\text{r},j}F_{\text{r},j}R_{\text{t},i}^2(k|k-1)R_{\text{r},j}^2(k|k-1)}, \tag{42}$$

Table 1
Radar Networks Parameters

Parameter	Value	Parameter	Value
G_t	37.5 dB	τ	10^{-6}
G_r	37.5 dB	B_r	1 MHz
$\sigma_j(\forall j)$	55 m^2	F_r	3 dB
σ_θ	50 mrad	λ	0.03 m
G_{RP}	45	$\overline{P_{max}}$	1 KW
$\overline{P_{min}}$	0	SNR_{min}	16.2 dB
T_r	10^{-3} s	$\overline{T_{max}}$	4×10^{-2} s

For simplicity, it is assumed that each transmitter-receiver pair combination in the networks is the same. Rearranging terms in (42) yields

$$SNR_c(k) = \frac{u_i(k)T_{d,i}(k)P_{t,i}(k)}{T_r B_r R_{t,i}^2(k|k-1)} \frac{G_t G_r \lambda^2 G_{RP}}{(4\pi)^3 k T_0 F_r} \sum_{j=1}^{N_r} \frac{\sigma_j}{R_{r,j}^2(k|k-1)}, \tag{43}$$

Since the minimum transmitting energy is achieved when the SNR in the network at each time step is equal to the predetermined SNR threshold, this gives

$$\frac{u_i(k)T_{d,i}(k)P_{t,i}(k)}{T_r B_r R_{t,i}^2(k|k-1)} C_1 \sum_{j=1}^{N_r} \frac{\sigma_j}{R_{r,j}^2(k|k-1)} = SNR_{min}, \tag{44}$$

where

$$C_1 = \frac{G_t G_r \lambda^2 G_{RP}}{(4\pi)^3 k T_0 F_r}. \tag{45}$$

Rearranging terms yields

$$u_i(k)P_{t,i}(k) = SNR_{min} \frac{T_r B_r R_{t,i}^2(k|k-1)}{T_{d,i}(k) C_1} \frac{1}{\sum_{j=1}^{N_r} \frac{\sigma_j}{R_{r,j}^2(k|k-1)}}. \tag{46}$$

Substituting (46) into (34), (34) can be rewritten as

$$p_I(k) = \frac{T_{d,i}(k)(T_{d,i}(k) + \tau_I)}{2T_I \Delta T(k)} \times \frac{1}{2} \mathrm{erfc}\left(\sqrt{-\ln p'_{fa}} - \sqrt{SNR_{min} \frac{T_r B_r C_2}{T_{d,i}(k) C_1} \frac{1}{\sum_{j=1}^{N_r} \frac{\sigma_j}{R_{r,j}^2(k|k-1)}} + \frac{1}{2}} \right), \tag{47}$$

where

$$C_2 = \frac{G_t G_I \lambda^2 G_{IP}}{(4\pi)^2 k T_0 B_I F_I}. \tag{48}$$

Let us define $a = \sqrt{-\ln p'_{fa}}$, $b = SNR_{min} \frac{T_r B_r C_2}{T_{d,i}(k) C_1} \frac{1}{\sum_{j=1}^{N_r} \frac{\sigma_j}{R_{r,j}^2(k|k-1)}}$, $x = T_{d,i}(k)$, $c = T_I \Delta T(k)$, $d = \tau_I$, then (47) can be described as

Table 2
Intercept Receiver Parameters

Parameter	Value	Parameter	Value
p'_{fa}	10^{-6}	G_{IP}	2 dB
F_I	6 dB	T_I	2 s
G_I	0 dB	B_I	40 GHz
c_v	3×10^8 m/s	M_I	50 MHz

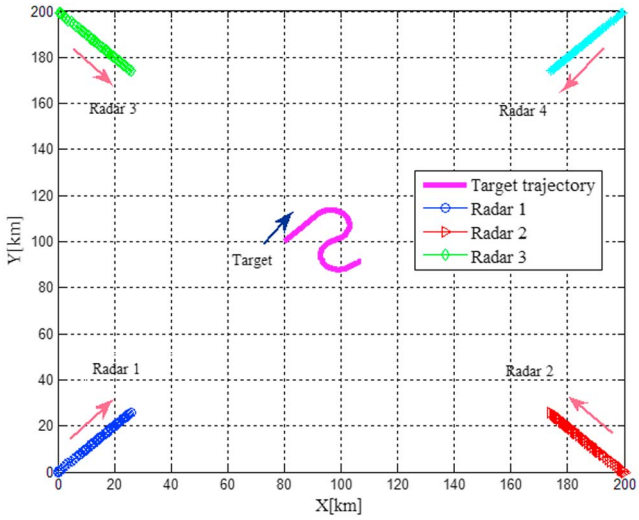

Figure 4. Deployment of radar networks with respect to the target in the simulations.

$$p_{\mathrm{I}}(x) = \frac{x(x+d)}{2c}\operatorname{erfc}\left(a - \sqrt{\frac{b}{x} + \frac{1}{2}}\right) = \frac{x(x+d)}{c}\left(\frac{1}{2} - \frac{1}{\sqrt{\pi}}\int_0^{a-\sqrt{\frac{b}{x}+\frac{1}{2}}} e^{-t^2} dt\right). \tag{49}$$

Subsequently, we obtain the second derivative of $p_{\mathrm{I}}(x)$ with respect to x as follows:

$$\frac{\partial^2 p_{\mathrm{I}}(x)}{\partial x^2} < 0, x \in [T_{\mathrm{r}}, \overline{T_{\max}}]. \tag{50}$$

The detailed proof can be found in Appendix A.

Thus, it can be concluded from (50) that the intercept probability is upper convex with respect to the dwell time (Boyd, 2004; Liu et al., 2015). Intuitively, the optimal point is always at the boundary, when $T_{\mathrm{d},i}(k) = T_{\mathrm{r}}$, or $T_{\mathrm{d},i}(k) = \overline{T_{\max}}$. That is to say, the minimum intercept probability p_{I} can be obtained at the boundary, that is,

$$T_{\mathrm{d},i}(k) = \arg\min\{p_{\mathrm{I}}(T_{\mathrm{r}}), p_{\mathrm{I}}(\overline{T_{\max}})\}. \tag{51}$$

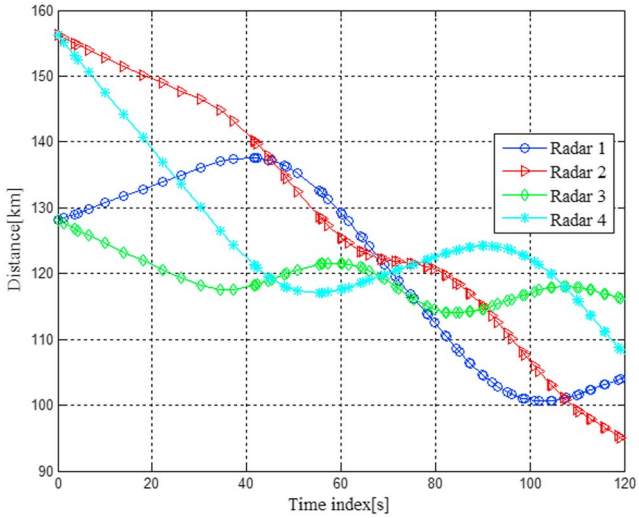

Figure 5. The distances between radars and target.

Moreover, the radar transmitter with the minimum transmission power $P_{t,i}(k)$ is selected based on (46):

$$i = \arg\min_{i\in\mathbb{S}} u_i(k)P_{t,i}(k) \tag{52}$$

The pseudo-code of the transmitter selection is summarized in Algorithm 1.

Algorithm 1 : Radar Transmitter Selection Algorithm

1: **initialize** $i = 1, \mathbb{S} = \{1, 2, \ldots, N_r\}$;
2: **while** $i \leq N_r$ **do**
$i = \arg\min_{i\in\mathbb{S}} u_i(k)P_{t,i}(k)$;
$i \leftarrow i + 1$;
3: **end**

Eventually, the value of $\mathrm{SNR}_{pre}(k)$ is utilized to compute the measurement noise covariance matrix $\mathbf{R}^i(k)$. Given $\mathbf{R}^i(k)$, the Kalman gain matrix $\mathbf{K}^i(k)$ can be computed according to (13).

Remark 4: As previously stated, the minimum intercept probability p_l can be obtained at the point $\min\{p_l(T_r), p_l(\overline{T_{max}})\}$. If $T_{d,i}(k) = \overline{T_{max}}$, the corresponding LPI strategy is called the minimum power strategy, in which case the selected radar transmitter radiate the minimum power at all times and uses maximum signal integration. The intent is always to stay below the intercept receiver threshold (Lynch, 2004). While if $T_{d,i}(k) = T_r$, the LPI strategy is known as the minimum dwell strategy, which is to keep the illumination time as short as possible. This means that the selected transmitter should be in its high power mode for the minimum time possible. Generally, the revisit interval, dwell time, transmitter selection, and transmit power should be optimized based on the real time status information in hostile environments, such that the LPI performance of a radar network can be improved.

3.4.3. Updating Target State with Obtained Measurements

According to the selection of the revisit interval and working parameters scheduling, the selected radar transmitter i must illuminate the target and produce a measurement $\mathbf{Z}^i(k)$ at the moment of $\Delta T(k)$, which is used to update the target state vector $\mathbf{X}(k|k)$ and associated error covariance $\mathbf{P}(k|k)$. The general steps of the proposed JTSRM strategy are given in Algorithm 2. The revisit interval for time index $k + 1$ is calculated on the next iteration of the proposed JTSRM strategy, at the **Step 2**.

Algorithm 2 : The General Steps of JTSRM Strategy

1: **Step 1:** Let $k = 1$, and assume initial JTSRM optimization results;
2: **Step 2:** Given the target state estimation $\hat{\mathbf{X}}_i(k-1|k-1)$, model probability $q(k|k-1)$, and associated error covariance matrix $\mathbf{P}_i(k-1|k-1)$ for time index $k-1$;
3: **Step 3:** Select the revisit interval $\Delta T(k)$ based on the required target tracking accuracy P_{th} and calculate the predicted target tracking accuracy based on (22) and (23);
4: **Step 4:** Calculate the dwell time $T_{d,i}(k)$, transmitter selection $u_i(k)$ and transmit power $P_{t,i}(k)$ according to (51) and (52) for time index k;
5: **Step 5:** Send the optimization results $\Delta T(k)$, $T_{d,i}(k)$, $u_i(k)$ and $P_{t,i}(k)$ to the system controller to form the probing scheme;
6: **Step 6:** Make a measurement $\mathbf{Z}(k)$ with the determined working parameters and update the estimation of the target state;
7: **Step 7:** Let $k \leftarrow k + 1$, and go to **Step 2**.

3.5. Summary and Remarks

3.5.1. Target State Estimation

In this subsection, the closed-form JTSRM framework is given for target tracking in a distributed radar network.

Overall speaking, the closed-loop JTSRM strategy can be described as follows. First, the target state at the current time index $k-1$ is obtained by utilizing IMM-EKF technique. Then, the predictive covariance matrix $\mathbf{P}^{IMM}_{pre}(k|k-1)$ is fed back, based on which the JTSRM optimization is implemented. Finally, the resource-scheduling results are sent back to guide the illumination strategy in the next time period, thereby rendering it a closed-loop system (Yan et al., 2016). The general steps of the proposed JTSRM strategy are given in Algorithm 2.

Table 3
The Description of Target Motion

Time index[s]	Target motion
0–5 s	Constant velocity
5–15 s	Left turn ($w_+ = 5$rad)
15–30 s	Constant velocity
30–70 s	Right turn ($w_- = -5$rad)
70–75 s	Constant velocity
75–112.5 s	Left turn ($w_+ = 5$rad)
112.5–120 s	Constant velocity

3.5.2. Remarks

In this subsection, several remarks related to the closed-loop JTSRM strategy are provided as follows.

Remark 5: It is noteworthy that only a single target is considered in this paper. Nevertheless, it can straightforwardly be extended to a multiple-target scenario, where it is assumed that the targets are widely separated in the surveillance area. Based on the algorithm proposed in Zhang et al. (2011), for a multiple-target case, the selected radar transmitter should illuminate and track the target whose predicted revisit interval is the smallest at the next time index. According to the optimized revised interval, dwell time and transmit power, the selected target's state and associated error covariance matrix can be updated with the obtained measurements, while other targets' states remain unchanged. Then, return to Step (1) to track the target whose revisit interval is the next smallest. Therefore, the problem of multiple-target tracking can be simplified as several single-target-tracking problems that can be solved independently. The conclusions obtained in this study suggest that similar LPI benefits would be achieved for the multiple-target case.

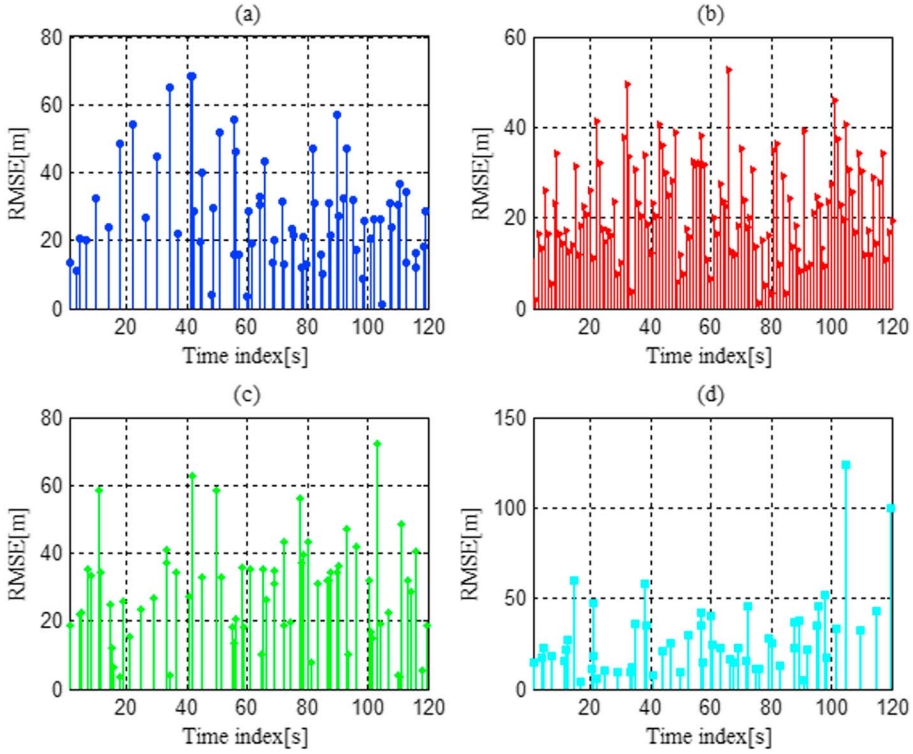

Figure 6. Target tracking RMSEs for different algorithms: (a) The proposed JTSRM strategy; (b) constant revisit interval algorithm; (c) the algorithm proposed by Chen J.; and (d) the algorithm proposed by Narykov A. S. RMSE = root-mean-square error; JTSRM = joint transmitter selection and resource management.

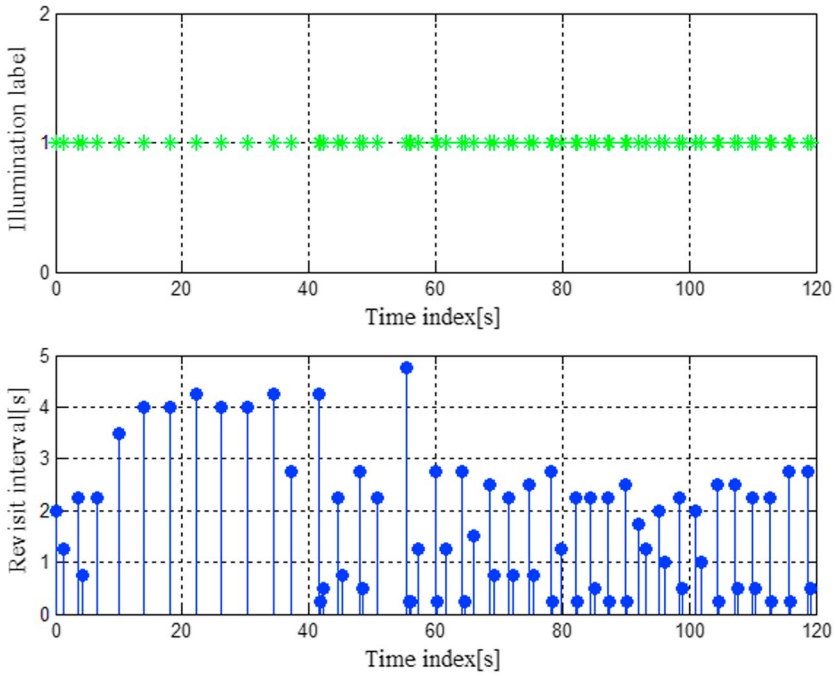

Figure 7. The illumination label and revisit interval $\Delta T(k)$ utilizing the proposed joint transmitter selection and resource management strategy.

Remark 6: In the proposed closed-loop JTSRM framework, the measurement model (7) is a highly nonlinear function. Thus, the IMM-EKF method is utilized as the tracker to obtain an accurate estimate of target state. It is worth to mention that other estimators such as particle filter can also be employed in this problem.

4. Numerical Results and Discussion

In this section, numerical simulation results are provided to verify the accuracy of the theoretical derivations and to demonstrate the superiority of the proposed JTSRM algorithm in terms of target tracking accuracy and LPI performance.

4.1. Numerical Description

A distributed radar network system with $N_R = 4$ spatially diverse radars is considered with corresponding key parameters of the system in Tables 1 and 2.

The deployment of radar networks with respect to the target in the simulations is presented in Figure 4, and the relative distances between radars and target are illustrated in Figure 5. The duration of the tracking is 120 s. The initial positions of the radars are located at (0,0) km, (200,0) km, (0,200) km, and (200,200) km, respectively. The radar nodes departure from their initial locations and follow the lines of different colors for the next 120 s. The initial target state is $\mathbf{X}(1) = [80\text{ km}, 400\text{ m/s}, 100\text{ km}, 400\text{ m/s}]$. The initial model probabilities are 0.3 for the target to be both in the constant velocity (CV) model $\mathbf{F}_{CV}$ and the coordinate turn model $\mathbf{F}_{CT}$ with $w_+ = 5$ rad, while the remaining 0.4 is for the target to be in the coordinate turn model $\mathbf{F}_{CT}$ with $w_- = -5$ rad. The trajectory consists of four CV segments and three turns. Table 3 shows the detailed description of target motion. The process noise intensity σ_w^2 is 25. The model transition probability matrix is set to be

$$\mathbf{P}_{\text{trans}} = \begin{bmatrix} 0.9 & 0.05 & 0.05 \\ 0.1 & 0.8 & 0.1 \\ 0.05 & 0.15 & 0.8 \end{bmatrix}, \tag{53}$$

which denotes a probability of a transition from one model to another. The initial error covariance matrix of the target state is $\mathbf{P}(1|1) = \text{diag}\{500, 15, 500, 15\}$. The revisit interval is selected from the set $\mathbf{\Omega} = 5$ s, 4.75 s, 4.5 s, 4.25 s, … , 0.25 s. The radars measure the relative ranges and azimuths of the target.

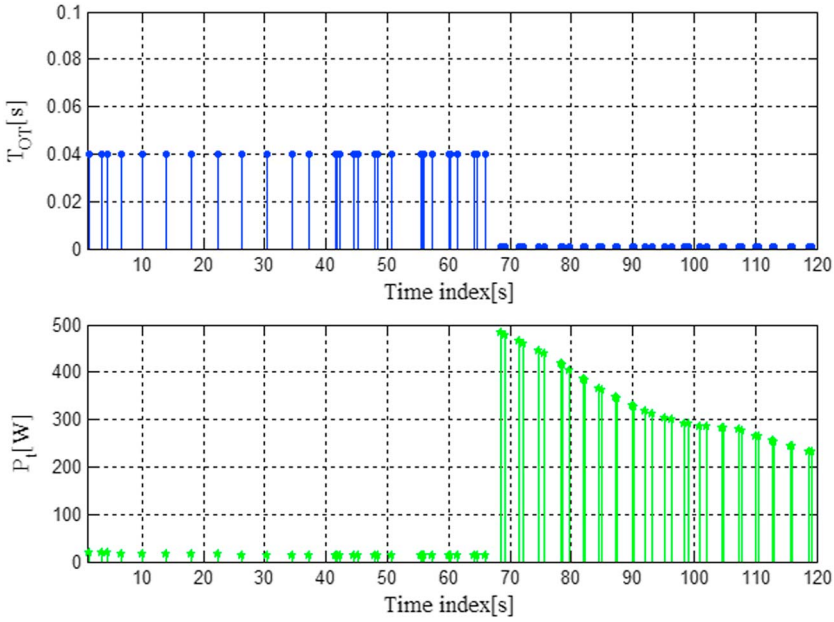

Figure 8. Transmitting parameters utilizing the proposed joint transmitter selection and resource management strategy. The plotted values are: dwell time $T_{d,i}(k)$ and transmit power $P_{t,i}(k)$ for the scheduled measurements.

4.2. Simulation Results

As mentioned before, the prediction accuracy in target position is selected to be the requirement that is applied on the predicted tracking performance by keeping only the elements related to target positional variances in (23). In this section, we set the threshold P_{tgh} for target tracking accuracy to be 2,500 m^2. At each time index, the proposed JTSRM optimization strategy is solved numerically. To better disclose the effects of our proposed scheme on the target tracking performance, Figure 6 depicts the root-mean-square error (RMSE) of target tracking averaged over 500 Monte Carlo trials. The RMSE at the kth tracking interval can be calculated as follows:

$$\mathrm{RMSE}(k) = \sqrt{\frac{1}{N_{MC}} \sum_{n=1}^{N_{MC}} \left\{ \left[x(k) - \hat{x}_n(k|k)\right]^2 + \left[y(k) - \hat{y}_n(k|k)\right]^2 \right\}}, \tag{54}$$

where N_{MC} is the number of Monte Carlo trials, $[\hat{x}_n(k|k), \hat{y}_n(k|k)]$ is the estimation of target state at the nth trial. It is worth pointing out that the revisit interval of the constant revisit interval algorithm is fixed at 1 s, which exhibits the smallest RMSE in target tracking. An intuitive explanation is that the selected transmitter is scheduled to illuminate the target with the maximum energy in each time index. In addition, the algorithms

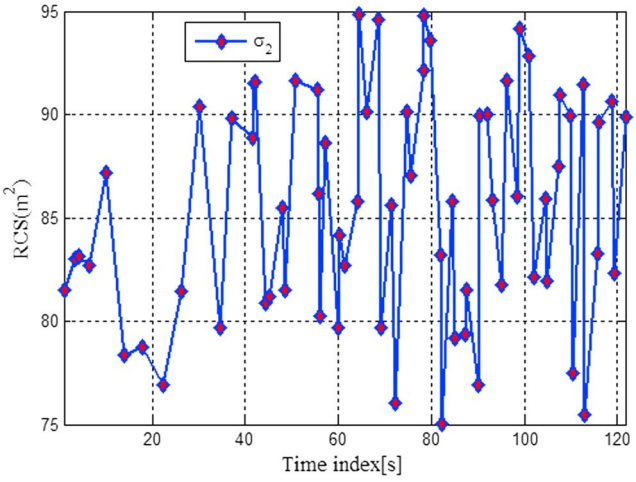

Figure 9. The second RCS model. RCS = radar cross section.

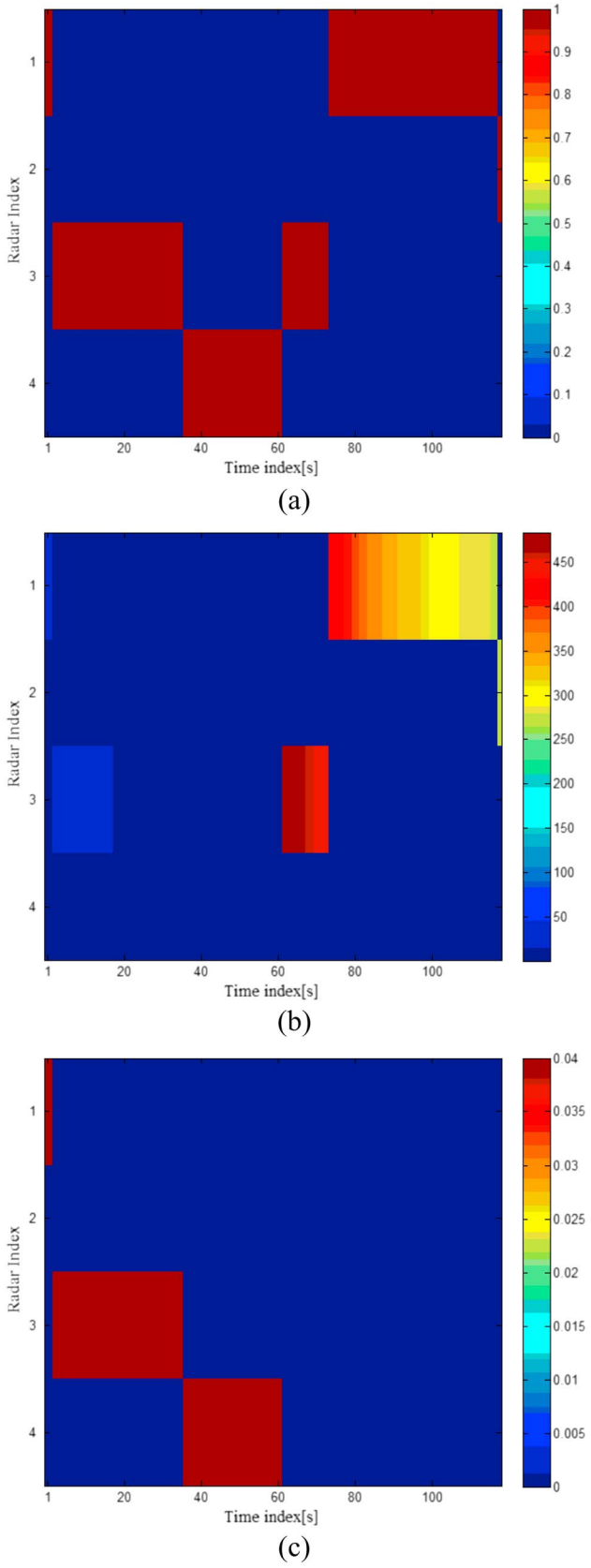

Figure 10. Joint transmitter selection and resource management optimization results in Case I: (a) Transmitter selection result; (b) transmit power result; and (c) dwell time result.

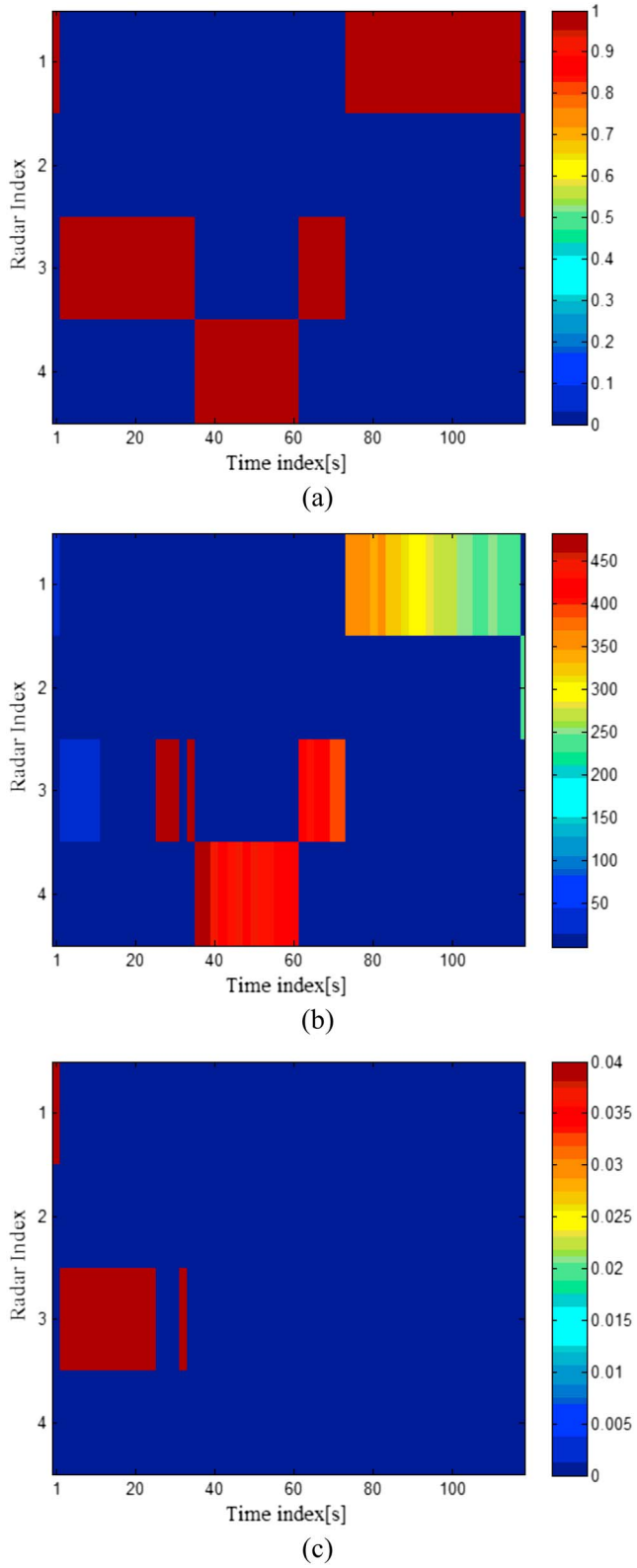

Figure 11. Joint transmitter selection and resource management optimization results in Case II: (a) Transmitter selection result; (b) transmit power result; and (c) dwell time result.

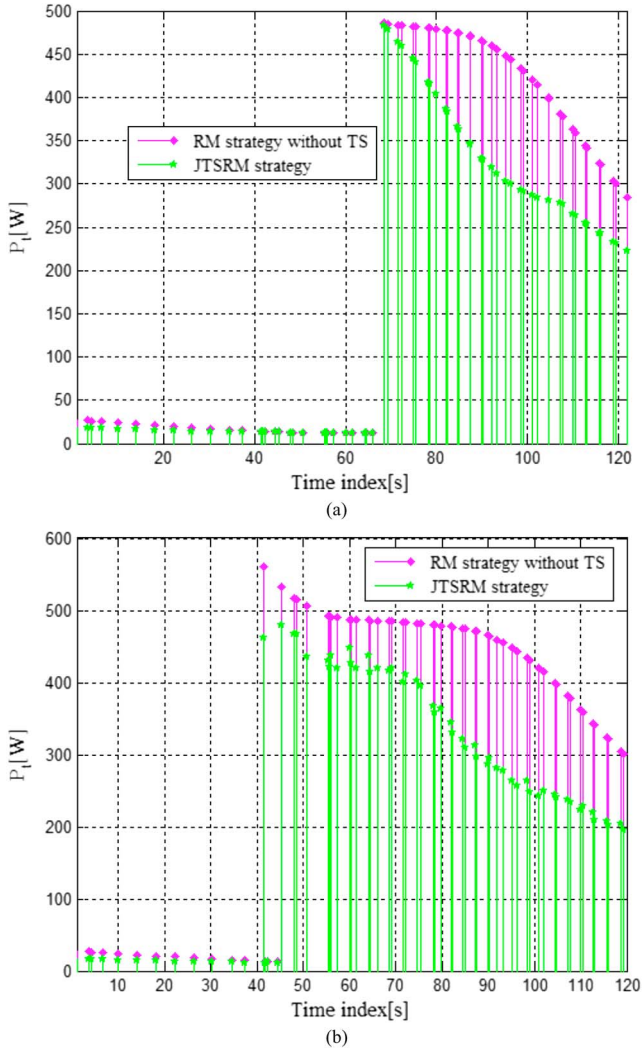

Figure 12. Comparisons of transmit power $P_{t,i}(k)$ with two algorithms: (a) Case I; (b) Case II. RM = resource management; TS = transmitter selection; JTSRM = joint transmitter selection and resource management.

presented in Chen et al. (2014) and Narykov et al. (2013) do not perform well compared to our proposed JTSRM strategy, which can maintain the predefined target tracking performance by optimizing the revisit interval, dwell time, and transmitted power. This confirms the superior target-tracking accuracy of the proposed strategy.

The illumination label and revisit interval utilizing the presented JTSRM optimization strategy are plotted in Figure 7. Since the proposed strategy starts with the selection of the revisit interval $\Delta T(k)$, this parameter is plotted first. One can observe that different values of revisit interval are selected at each step of target tracking. The results in Figure 7 reveal that the proposed scheme can save up to 38.3% of the total times of radar illumination as compared to the constant revisit interval method. As expected, the revisit interval is not necessary to be 1 s all the time to maintain the specified target-tracking performance. Specifically, during the target-nonmaneuvering period, the revisit interval can be selected as large as 4.75 s. Most time it is much larger than 1 s, thereby reducing the consumed time resource on target tracking. Patterns of the optimized transmitting parameters for radar network, obtained from a single Monte Carlo simulation run, are shown in Figure 8, where either the minimum power strategy or the minimum dwell strategy is selected based on the real time target status information in the target-tracking process. For the period 0–66 s, the selected radar transmitter illuminates the target with the longest dwell time, while the maximum power strategy is selected between 68.5 s and 120 s, during which the transmitter is scheduled to radiate the largest power as the target

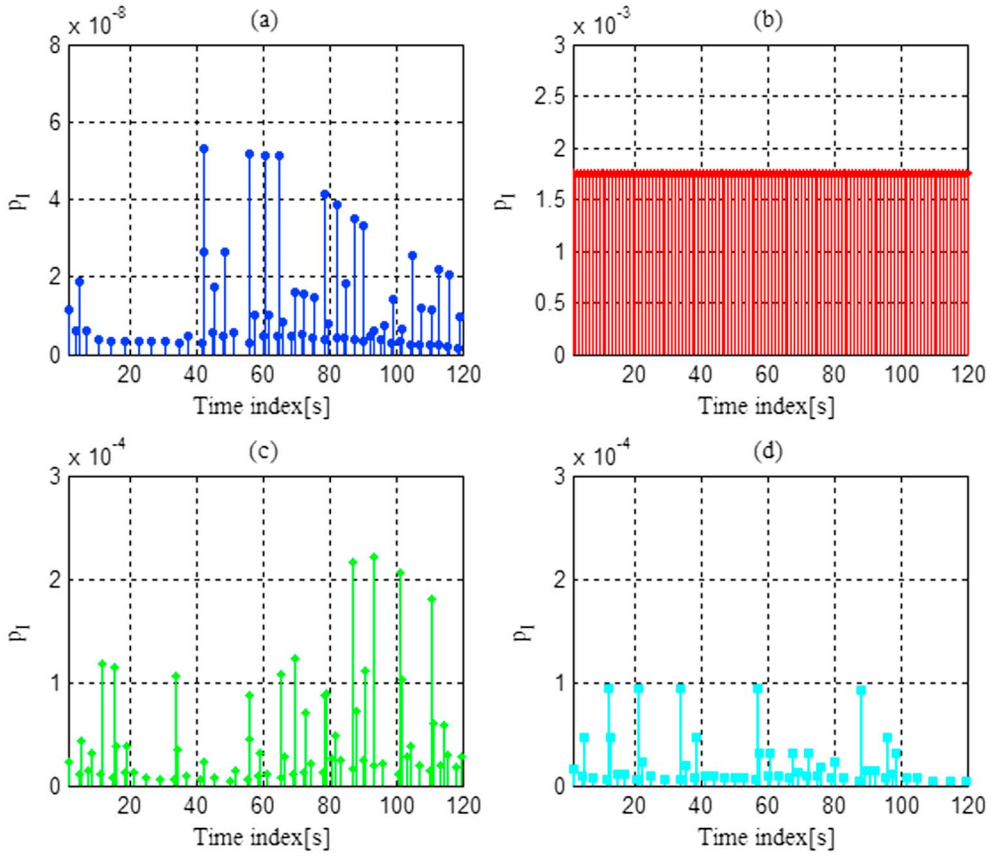

Figure 13. The values of intercept probability $p_I(k)$ for different algorithms in Case I: (a) The proposed joint transmitter selection and resource management strategy; (b) constant revisit interval algorithm; (c) the algorithm proposed by Chen J.; (d) the algorithm proposed by Narykov A. S.

is flying away from the radar network. The dwell time and transmitted power are adaptively optimized to minimize the LPI performance criterion in (35), providing the improved LPI performance in the radar network.

In order to better evaluate the effect of the target RCS on the JTSRM optimization results, we consider two different RCS models, which are defined as follows:

$$\begin{cases} \text{Case I:}\sigma_j = 55\text{m}^2, \forall j \\ \text{Case II:}\sigma_j = 55\text{m}^2, \forall j \neq 2 \end{cases} \tag{55}$$

It is worth pointing out that Case I supports the evaluation of resource management with the target RCS being factored out, leaving only the system geometry to affect optimization results (Xie et al., 2018). In Case II, the target RCS with respect to radar 2 is illustrated in Figure 9, while other RCS parameters are kept the same as Case I.

Here we investigate the above two cases, and the corresponding optimization results are shown separately in Figures 10 and 11. In Figure 10a, the blue areas in each time index mean that the transmitter selection variable $u_i(k) = 0$, while the red areas indicate that $u_i(k) = 1$. The different colors in Figures 10b and 10c represent the values of dwell time and transmitted power. As shown in Figure 10, at initial time $t = 1$ s, there are no prior knowledge. Thus, the radar node 1 is primarily selected to illuminate the target. For 1 s $< t <$ 19 s, radar 3 is selected to track the target with the optimized dwell time and transmit power, which is due to the fact that this node is relatively closer and has better angular spread with respect to the target. From Figure 11 we can observe that the transmitter selection result is not changed, whereas the working parameters have correspondingly changed. Thus, it can be concluded that the JTSRM strategy depends not only on the relative geometry between target and radar networks but also on the target reflectivity.

Moreover, Figures 12a and 12b illustrate the comparisons of transmit power in two cases by utilizing the proposed JTSRM strategy and the adaptive resource management (RM) strategy without transmitter selection (TS) in Shi et al., (2017; where radar 4 is taken as the dedicated radar transmitter), respectively. The results imply that the JTSRM strategy can minimize the transmit power by selecting the optimal node to radiate radar signals.

In order to illustrate the superiority of the proposed JTSRM strategy on the LPI performance in a radar network, Figure 13 compares the values of intercept probability $p_l(k)$ for different algorithms in Case I. Analyzing the results in Figure 11a together with the plot in Figure 13b corresponding to the scenario of a radar network with constant transmitting parameters, we can see that the presented strategy can significantly improve the LPI performance of a radar network, where the intercept probability of the radar network with fixed transmitting parameters keeps constant 1.75×10^{-3} during the whole target-tracking process. One can also notice from Figure 13c that the LPI performance employing the algorithm proposed by Chen J. is significantly worse than that of the proposed JTSRM strategy, in which only the revisit interval is optimized to minimize the total number of radar radiation for a given target-tracking accuracy, and the values of $p_l(k)$ are much larger than those in Figure 13a during the target-tracking period. Also, the LPI performance of the transmitting parameters selection algorithm in Narykov et al. (2013) is inferior to that of the presented strategy. The reason is that the former aims to improve the LPI performance by optimizing the revisit interval and the dwell time while the transmitted power remains constant. It is apparent that the value of intercept probability $p_l(k)$ utilizing the proposed JTSRM strategy is strictly smaller than the other algorithms, which confirms the LPI performance improvement by exploiting the presented scheme in a radar network. As mentioned before, this is due to the fact that at each time index the radar transmitting parameters, in terms of the revisit interval, dwell time, transmitter selection, and transmission power, are adaptively optimized to enhance the LPI performance for a radar network. Therefore, it can be concluded that the JTSRM optimization algorithm is able to adjust the working parameters to deal with the change in target dynamics, hence leading to the optimum LPI performance.

5. Conclusions and Future Work

The main contribution in the present work is to propose a JTSRM strategy for target tracking in distributed radar networks. The basis of this strategy is to utilize the optimization technique to minimize the LPI performance criterion of radar networks by optimizing the revisit interval, dwell time, transmitter selection, and transmit power for a desired target-tracking performance. The resulting optimization problem was solved through a developed three-step solution method. Simulation results have been provided to demonstrate the effectiveness of the JTSRM strategy, the correctness of the closed-loop JTSRM framework, and the efficiency of the presented three-step solution. It was also shown that the JTSRM optimization results depend not only on the relative geometry between target and radar networks but also on the target reflectivity.

To generalize the presented JTSRM strategy, our future work is to study the JTSRM algorithm for multitarget tracking in radar networks. In addition, the effectiveness of the strategy in the presence of target birth and death will be part of our future work and investigation.

Appendix A: Proof of the Upper Convexity of Intercept Probability With Respect to the Dwell Time

Taking the first derivative of $p_l(k)$ with respect to x, we can observe that

$$\frac{\partial p_l(x)}{\partial x} = \frac{1}{4}\frac{e^{-(a-\frac{\sqrt{2}}{2}\sqrt{\frac{2b+x}{x}})^2}\sqrt{2}(\frac{1}{x}-\frac{2b+x}{x^2})x(x+d)}{\sqrt{\pi}\sqrt{\frac{2b+x}{x}}c} + \frac{2x+d}{c}\left[\frac{1}{2}-\frac{1}{2}\mathrm{erf}\left(a-\frac{\sqrt{2}}{2}\sqrt{\frac{2b+x}{x}}\right)\right], \tag{A1}$$

$$\mathrm{erf}(z) = \frac{2}{\sqrt{\pi}}\int_0^z e^{-v^2}\mathrm{d}v. \tag{A2}$$

From (1.1) it should be noted that the extreme point cannot be obtained by setting $\frac{\partial p_l(x)}{\partial x} = 0$. Then, we take the second derivative of $p_l(x)$ with respect to x as follows:

$$\begin{aligned}\frac{\partial^2 p_l(x)}{\partial x^2} = \frac{1}{4}\frac{1}{(2b+x)\sqrt{\pi}c}\left[\left(a-\frac{\sqrt{2}}{2}\sqrt{\frac{2b+x}{x}}\right)x^2(x+d)\left(\frac{1}{x}-\frac{2b+x}{x^2}\right)^2\right.\\ \left.\times e^{-\left(a-\frac{\sqrt{2}}{2}\sqrt{\frac{2b+x}{x}}\right)^2}\right]+\frac{1}{4}\frac{e^{-\left(a-\frac{\sqrt{2}}{2}\sqrt{\frac{2b+x}{x}}\right)^2}\sqrt{2}\left[-\frac{2}{x^2}+\frac{2(2b+x)}{x^3}x(x+d)\right]}{\sqrt{\pi}\sqrt{\frac{2b+x}{x}}c}\\ +\frac{1}{2}\frac{e^{-\left(a-\frac{\sqrt{2}}{2}\sqrt{\frac{2b+x}{x}}\right)^2}\sqrt{2}(2x+d)\left(\frac{1}{x}-\frac{2b+x}{x^2}\right)}{\sqrt{\pi}\sqrt{\frac{2b+x}{x}}c}\\ +\frac{1}{c}\left[1-\mathrm{erf}\left(a-\frac{\sqrt{2}}{2}\sqrt{\frac{2b+x}{x}}\right)\right]\\ -\frac{1}{8}\frac{e^{-\left(a-\frac{\sqrt{2}}{2}\sqrt{\frac{2b+x}{x}}\right)^2}\sqrt{2}\left(\frac{1}{x}-\frac{2b+x}{x^2}\right)^2x(x+d)}{\sqrt{\pi}\left(\frac{2b+x}{x}\right)^{\frac{3}{2}}c}.\end{aligned} \tag{A3}$$

After basic algebraic manipulations in Liu et al. (2015), we can obtain

$$\begin{aligned}\frac{\partial^2 p_l(x)}{\partial x^2} &= -\frac{b^2}{(2b+x)^{\frac{3}{2}}\sqrt{\pi}cx^{\frac{5}{2}}}e^{-\left(a-\frac{\sqrt{2}}{2}\sqrt{\frac{2b+x}{x}}\right)^2}\left(\sqrt{2}b+\sqrt{2}ax-\sqrt{x}\sqrt{2b+x}\right)(x+d)\\ &\quad-\frac{\sqrt{2}\frac{b}{x}e^{-\left(a-\frac{\sqrt{2}}{2}\sqrt{\frac{2b+x}{x}}\right)^2}}{\sqrt{\pi}\sqrt{\frac{2b+x}{x}}c}+\frac{1}{c}\left[1-\mathrm{erf}\left(a-\frac{\sqrt{2}}{2}\sqrt{\frac{2b+x}{x}}\right)\right]\\ &= \underbrace{-\frac{b^2(x+d)}{(2b+x)^{\frac{3}{2}}\sqrt{\pi}cx^{\frac{5}{2}}}e^{-\left(a-\frac{\sqrt{2}}{2}\sqrt{\frac{2b+x}{x}}\right)^2}\left(\sqrt{2}b+\sqrt{2}ax-\sqrt{x}\sqrt{2b+x}\right)}_{<0}\\ &\quad\underbrace{-\frac{\sqrt{2}\frac{b}{x}e^{-\left(a-\frac{\sqrt{2}}{2}\sqrt{\frac{2b+x}{x}}\right)^2}}{\sqrt{\pi}\sqrt{\frac{2b+x}{x}}c}}_{<0}+\frac{1}{c}\left[1-\mathrm{erf}\left(a-\frac{\sqrt{2}}{2}\sqrt{\frac{2b+x}{x}}\right)\right]\end{aligned} \tag{A4}$$

1. It is apparent from (A4) that whether the first term of $\frac{\partial^2 p_l(x)}{\partial x^2}$ is positive or not is determined by $(\sqrt{2}b+\sqrt{2}ax-\sqrt{x}\sqrt{2b+x})$. Here we define

$$f(x,a,b) = \sqrt{2}b+\sqrt{2}ax-\sqrt{x}\sqrt{2b+x}. \tag{A5}$$

It is assumed that $f(x,a,b)>0$. Then, we can obtain that

$$\sqrt{2}b+\sqrt{2}ax+\sqrt{x}\sqrt{2b+x}>0. \tag{A6}$$

which is equivalent to the following equation:

$$\begin{aligned}&\left(\sqrt{2}b+\sqrt{2}ax+\sqrt{x}\sqrt{2b+x}\right)\left(\sqrt{2}b+\sqrt{2}ax-\sqrt{x}\sqrt{2b+x}\right)\\ &=\left(\sqrt{2}b+\sqrt{2}ax\right)^2-\left(\sqrt{x}\sqrt{2b+x}\right)^2\\ &=(2a^2-1)x^2+(4ab-2b)x+2b^2>0.\end{aligned} \tag{A7}$$

It is known to us all that the equation $ax^2 + bx + c = 0$ has real solutions, if and only if $\Delta = b^2 - 4ac \geq 0$. Owing to

$$\begin{aligned}\Delta &= (4ab - 2b)^2 - 4(2a^2 - 1) \times 2b^2 \\ &= -4b^2(4a - 3),\end{aligned} \tag{A8}$$

while $a = \sqrt{-\ln p'_{fa}} \in [\sqrt{\ln 10^3}, \sqrt{\ln 10^{12}}] \approx [2.628, 5.237]$, we have

$$\Delta = -4b^2(4a - 3) < 0. \tag{A9}$$

Thus, we obtain that the equation $(2a^2 - 1)x^2 + (4ab - 2b)x + 2b^2 = 0$ has no real solutions and $2a^2 - 1 > 0$, which means that $(2a^2-1)x^2+(4ab-2b)x+2b^2 > 0$ holds all the time. Moreover, from (A7) together with (A6), we can conclude that the inequality $f(x, a, b) > 0$ holds all the time. Hence, the first term in (A4) is negative.

2. Obviously, the second term in (A4) is negative.
3. The third term in (A4) can be expanded by employing Hans Heinrich Burmann's Theorem (Schopf & Supancic, 2014) as follows:

$$\begin{aligned}&\frac{1}{c}\left[1 - \operatorname{erf}\left(a - \frac{\sqrt{2}}{2}\sqrt{\frac{2b+x}{x}}\right)\right] \\ &\approx \frac{1}{c}\left[1 - \frac{2}{\sqrt{\pi}}\left(1 + e^{-\left(a-\frac{\sqrt{2}}{2}\sqrt{\frac{2b+x}{x}}\right)^2}\right)^{\frac{1}{2}}\right. \\ &\left.\times\left(\frac{\pi}{2} + \frac{31}{100}e^{-\left(a-\frac{\sqrt{2}}{2}\sqrt{\frac{2b+x}{x}}\right)^2} - \frac{341}{1000}e^{-2\left(a-\frac{\sqrt{2}}{2}\sqrt{\frac{2b+x}{x}}\right)^2}\right)\right]\end{aligned} \tag{A10}$$

$$\begin{aligned}&< \frac{1}{c}\left[1 - \frac{2}{\sqrt{\pi}}\left(\frac{\pi}{2} + \frac{31}{100}e^{-\left(a-\frac{\sqrt{2}}{2}\sqrt{\frac{2b+x}{x}}\right)^2} - \frac{341}{1000}e^{-2\left(a-\frac{\sqrt{2}}{2}\sqrt{\frac{2b+x}{x}}\right)^2}\right)\right] \\ &= \frac{1}{c}\left[1 - 1 - \frac{2}{\sqrt{\pi}}\left(\frac{31}{100}e^{-\left(a-\frac{\sqrt{2}}{2}\sqrt{\frac{2b+x}{x}}\right)^2} - \frac{341}{1000}e^{-2\left(a-\frac{\sqrt{2}}{2}\sqrt{\frac{2b+x}{x}}\right)^2}\right)\right] \\ &= \frac{2}{\sqrt{\pi}c}\left(\frac{31}{100}e^{-\left(a-\frac{\sqrt{2}}{2}\sqrt{\frac{2b+x}{x}}\right)^2} - \frac{341}{1000}e^{-2\left(a-\frac{\sqrt{2}}{2}\sqrt{\frac{2b+x}{x}}\right)^2}\right) < 0,\end{aligned} \tag{A11}$$

Thus, the third term in (A4) is negative as well. Subsequently, we can obtain the second derivative of $p_l(x)$ with respect to x as follows:

$$\frac{\partial^2 p_l(x)}{\partial x^2} < 0, x \in [T_r, \overline{T_{max}}]. \tag{A12}$$

Acknowledgments
We note that there are no data-sharing issues since all of the numerical information is provided in the figures, which are realized by MATLAB software. The MATLAB programs and numerical data are available as supporting information. This research is supported by the National Natural Science Foundation of China (grants 61371170 and 61671239), the Natural Science Foundation of Jiangsu Province (grant SBK2018041336), the Fundamental Research Funds for the Central Universities (grants NP2015404 and NS2016038), the National Aerospace Science Foundation of China (grants 20172752019 and 2017ZC52036), the Priority Academic Program Development of Jiangsu Higher Education Institutions (PADA) and Key Laboratory of Radar Imaging and Microwave Photonics (Nanjing Univ. Aeronaut. Astronaut.), Ministry of Education, Nanjing University of Aeronautics and Astronautics, Nanjing, 210016, China. In particular, the author Chenguang Shi would like to highlight the unwavering and invaluable support of his wife, Ying Hu.

References

Blair, W. D., Watson, G. A., Kirubarajan, T., & Bar-Shalom, Y. (1998). Benchmark for radar allocation and tracking in ECM. *IEEE Transactions on Aerospace and Electronic Systems*, *34*(4), 1097–1114.

Boers, Y., Driessen, H., & Zwaga, Z. H. (2006). Adaptive MFR parameter control: Fixed against variable probabilities of detection, IEE Proceedings-Radar. *Sonar and Navigation*, *153*(1), 2–6.

Boyd, S. P. (2004). *Convex optimization*. Cambridge: Cambridge University Press.

Chen, Y. F., Nijsure, Y., Yuen, C., Chew, Y. H., Ding, Z., & Boussakta, S. (2013). Adaptive distributed MIMO radar waveform optimization based on mutual information. *IEEE Transactions on Aerospace and Electronic Systems*, *49*(2), 1374–1385.

Chen, J., Wang, F., Zhou, J. J., & Shi, C. (2014). A novel radar radiation control strategy based on passive tracking in multiple aircraft platforms. In *IEEE China Summit and International Conference on Signal and Information Processing (ChinaSIP)* (pp. 777–780). Xi'an, China.

Cheng, T., Zou, D. Q., & He, Z. S. (2013). Adaptive waveform and sampling interval tracking based on estimation accuracy for Doppler radar (pp. 1–4). *IET International Radar Conference*, Xi'an, China.

Daeipour, E., Bar-Shalom, Y., & Li, X. (1994). Adaptive beam pointing control of a phased array radar using an IMM estimator. In *Proceedings of the American Control Conference* (pp. 2093–2097). Baltimore, MA.

Fisher, E., Haimovich, A., Blum, R. S., Cimini, L. J., Chizhik, D., & Valenzuela, R. A. (2006). Spatial diversity in radars-models and detection performance. *IEEE Transactions on Signal Processing*, *54*(3), 823–836.

Godrich, H., Tajer, A., & Poor, H. V. (2012). Distributed target tracking in multiple widely separated radar architectures. In *IEEE 7th Sensor Array and Multichannel Signal Processing Workshop (SAM)* (pp. 153–156). Hoboken, NJ.
Haimovich, A. M., Blum, R. S., & Cimini, L. J. Jr. (2008). MIMO radar with widely separated antennas. *IEEE Signal Processing Magazine*, *25*(1), 116–129.
Kalandros, M., & Pao, L. Y. (2002). Covariance control for multisensor systems. *IEEE Transactions on Aerospace and Electronic Systems*, *38*(2), 1138–1157.
Kelly, S. W., Noone, G. P., & Perkins, J. E. (1996). Synchronization effects on probability of pulse train interception. *IEEE Transactions on Aerospace and Electronic Systems*, *32*(1), 213–220.
Kershaw, D. J., & Evans, R. J. (1994). Optimal waveform selection for tracking systems. *IEEE Transactions on Information Theory*, *40*(5), 1536–1550.
Keuk, G. V., & Blackman, S. S. (1993). On phased-array radar tracking and parameter control. *IEEE Transactions on Aerospace and Electronic Systems*, *29*(1), 186–194.
Kirubarajan, T., Bar-Shalom, Y., Blair, W. D., & Watson, G. A. (1998). IMMPDAF for radar management and tracking benchmark with ECM. *IEEE Transactions on Aerospace and Electronic Systems*, *34*(4), 1115–1134.
Li, J., & Stoica, P. (2009). *MIMO radar signal processing*. Hoboken, NJ: Wiley.
Liu, H. Q., Wei, X. Z., Li, F., et al. (2015). The real time control method of radar single radiation power based on RF stealth at the tracking. *ACTA ELECTRONICA SINICA*, *43*(10), 2047–2052.
Lynch, D. Jr. (2004). *Introduction to RF stealth*. Raleigh, NC: SciTech Publishing.
Mahafza, B. R., & Elsherbeni, A. Z. (2009). *MATLAB simulations for radar systems design*. Beijing: Publishing House of Electronics Industry.
Naghsh, M. M., Mahmoud, M. H., Shahram, S. P., Soltanalian, M., & Stoica, P. (2013). Unified optimization framework for multi-static radar code design using information-theoretic criteria. *IEEE Transactions on Signal Processing*, *61*(21), 5401–5416.
Narykov, A. S., Krasnov, O. A., & Yarovoy, A. (2013). Algorithm for resource management of multiple phased array radars for target tracking. In *The 16th International Conference on Information Fusion* (pp. 1258–1264). Istanbul, Turkey.
Narykov, A. S., & Yarovoy, A. (2013). Sensor selection algorithm for optimal management of the tracking capability in multisensor radar system. In *Proceedings of the 43rd European Microwave Conference* (pp. 1811–1196). Nuremberg, Germany.
Nguyen, N. H., Dogancay, K., & Davis, L. M. (2015). Adaptive waveform selection for multistatic target tracking. *IEEE Transactions on Aerospace and Electronic Systems*, *51*(1), 688–700.
Niu, R. X., Blum, R. S., Varshney, P. K., & Drozd, A. L. (2012). Target localization and tracking in noncoherent multiple-input multiple-output radar systems. *IEEE Transactions on Aerospace and Electronic Systems*, *48*(2), 1466–1489.
Pace, P. E. (2009). *Detecting and classifying low probability of intercept radar*. Boston: Artech House.
Puranik, S. P., & Tugnait, J. K. (2005). On adaptive sampling for multisensor tracking of a maneuvering target using IMM/PDA filtering. In *Proceedings of the American Control Conference* (pp. 1263–1268). Portland, OR.
Schleher, D. C. (2006). LPI radar: Fact or fiction. *IEEE Aerospace and Electronic Systems Magazine*, *21*(5), 3–6.
Schopf, H. M., & Supancic, P. H. (2014). On Burmann's theorem and its application to problems of linear and nonlinear heat transfer and diffusion. *The Mathematica Journal*, *16*, 1–44.
Self, A. G., & Smith, B. G. (1985). Intercept time and its prediction. *IEE proceedings F (Communications Radar and Signal Processing)*, *132*(4), 215–220.
She, J., Wang, F., & Zhou, J. J. (2016). A novel sensor selection and power allocation algorithm for multiple-target tracking in an LPI radar networks. *Sensors*, *16*, 2193. https://doi.org/10.3390/s16122193
She, J., Zhou, J. J., Wang, F., & Li, H. (2017). LPI optimization framework for radar network based on minimum mean-square error estimation. *Entropy*, *19*, 397. https://doi.org/10.3390/e19080397
Shi, C. G., Wang, F., Sellathurai, M., & Zhou, J. (2016). Transmitter subset selection in FM-based passive radar networks for joint target parameter estimation. *IEEE Sensors Journal*, *16*(15), 6043–6052.
Shi, C. G., Wang, F., Sellathurai, M., & Zhou, J. (2014). LPI optimization framework for target tracking in radar network architectures using information-theoretic criteria. *International Journal of Antennas and Propagation*, *2014*, 1–10.
Shi, C. G., Wang, F., Sellathurai, M., Zhou, J., & Salous, S. (2018). Power minimization-based robust OFDM radar waveform design for radar and communication systems in coexistence. *IEEE Transactions on Signal Processing*, *66*(5), 1316–1330.
Shi, C. G., Zhou, J. J., & Wang, F. (2016). LPI based resource management for target tracking in distributed radar network. In *2016 IEEE Radar Conference (RadarConf)* (pp. 822–826). Philadelphia, PA.
Shi, C. G., Zhou, J. J., & Wang, F. (2017). Adaptive resource management algorithm for target tracking in radar network based on low probability of intercept. *Multidimensional Systems and Signal Processing*, 1–24. https://doi.org/10.1007/s11045-017-0494-8
Sira, S. P., Papandreou-Suppappola, A., & Morrel, D. (2007). Dynamic configuration of time-varying waveforms for agile sensing and tracking in clutter. *IEEE Transactions on Signal Processing*, *55*(7), 3207–3217.
Song, X. F., Willett, P., & Zhou, S. L. (2012). Optimal power allocation for MIMO radars with heterogeneous propagation losses. In *IEEE International Conference on Acoustics Speech and Signal Processing (ICASSP)* (pp. 2465–2468). Kyoto, Japan.
Teng, Y., Griffiths, H. D., Baker, C. J., & Woodbridge, K. (2007). Netted radar sensitivity and ambiguity. *IET Radar Sonar and NavigationIET Radar, Sonar and Navigation*, *1*(6), 479–486.
Wang, X. L., Yi, W., Xie, M. C., Zhai, B., & Kong, L. (2017). Time management for target tracking based on the predicted Bayesian Cramer-Rao lower bound in phase array radar system. In *International Conference on Information Fusion* (pp. 1–5). Xi'an, China.
Wiley, R. G. (2006). *ELINT: The interception and analysis of radar signals*. Boston: Artech House.
Xie, M. C., Yi, W., Kirubarajan, T., & Kong, L. (2018). Joint node selection and power allocation strategy for multitarget tracking in decentralized radar networks. *IEEE Transactions on Signal Processing*, *66*(3), 729–743.
Yan, J. K., Liu, H. W., Pu, H. Q., Zhou, S., Liu, Z., & Bao, Z. (2016). Joint beam selection and power allocation for multiple target tracking in netted colocated MIMO radar system. *IEEE Transactions on Signal Processing*, *64*(24), 6417–6427.
Zhang, Z. K., Salous, S., Li, H. L., & Tian, Y. (2015). Optimal coordination method of opportunistic array radars for multi-target-tracking-based radio frequency stealth in clutter. *Radio Science*, *50*, 1187–1196. https://doi.org/10.1002/2015RS005728
Zhang, Z. K., & Tian, Y. B. (2016). A novel resource scheduling method of netted radars based on Markov decision process during target tracking in clutter. *EURASIP Journal on Advances in Signal Processing*, *2016*(16), 1–9.
Zhang, Z. K., Zhou, J. J., Wang, F., Liu, W., & Yang, H. (2011). Multiple-target tracking with adaptive sampling intervals for phased-array radar. *Journal of Systems Engineering and Electronics*, *22*(5), 760–766.
Zwaga, Z. H., Boers, Y., & Driessen, H. (2003). On tracking performance constrained MFR parameter control. In *Proceedings of the Sixth International Conference of Information Fusion* (pp. 712–718). Cairns, Queensland, Australia.